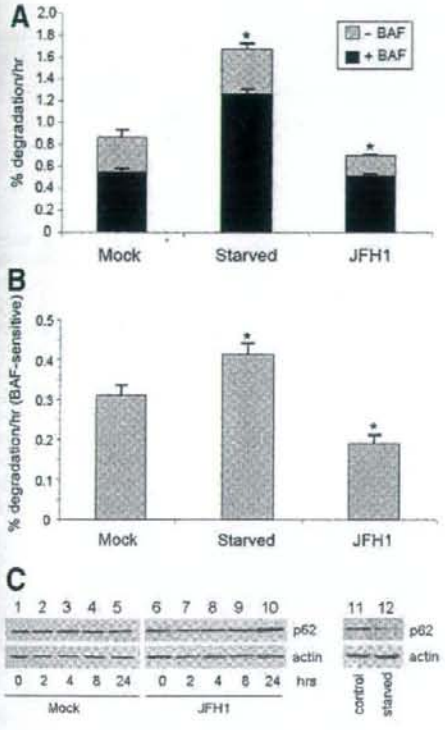

Fig. 3. Lack of enhancement of autophagic degradation by HCV. (A) and (B) The long-lived protein degradation assay. Mock, mock-transfected cells; Starved, nutrient-starved cells; JFH1, HCV JFH1 RNA transfected cells. The overall protein degradation rates in the absence (gray bar) or in the presence (black bar) of BAF are shown in A, and the BAF-sensitive protein degradation rates are highlighted in B. Asterisks indicate statistical significance ($P < 0.05$) when nutrient-starved cells or HCV JFH1 cells were compared against mock-transfected cells by Student *t* test. (C) Western blot analysis of p62/SQSTM1. Mock-transfected (lanes 1-5) or HCV JFH1 RNA transfected (lanes 6-10) cells were lysed at 0, 2, 4, 8, and 24 hours posttransfection for p62/SQSTM1 analysis using the anti-p62 antibody (American Research Products, Belmont, MA). Naïve Huh7.5 cells without (lane 11) or with nutrient starvation (lane 12) for 20 minutes were also analyzed. Actin was also analyzed to serve as a loading control. The p62 level in lane 12 was approximately 35% of that in lane 11 after normalization against actin.

To further investigate why the accumulation of autophagosomes induced by HCV did not lead to a higher protein degradation rate, we analyzed the level of autolysosomes in cells by staining stable GFP-LC3 cells with LysoTracker-red, which stains for acidic organelles such as lysosomes. GFP-LC3 cells that were starved for nutrients were used as a positive control. Bright GFP puncta (in other words, autophagic vacuoles) were detected in a large fraction of cells that were nutrient-starved (Fig. 4). Nearly half (colocalization coefficient 0.43) of these GFP puncta were also positive for LysoTracker-red. In contrast, when HCV cells were also analyzed, the fraction of GFP-LC3 puncta that was also positive for LysoTracker-red was significantly lower, with a colocalization coefficient of only 0.14 ($P < 0.005$). These results, together with the low autophagic protein degradation rate of HCV cells, indicated that the fusion between autophagosomes and lysosomes was inefficient in HCV cells.

Induction of ER Stress by HCV. Several HCV gene products, as well as the subgenomic RNA replicon, have been shown to induce ER stress, although sometimes with conflicting results.[15-18] Because ER stress has been shown to induce autophagy,[19,20] we decided to investigate whether HCV could induce the accumulation of autophagosomes via the induction of ER stress. We first examined whether HCV could induce ER stress during productive replication. ER stress, which is caused by the accumulation of misfolded proteins in the ER, can activate the UPR via three different sensors: PERK, ATF6, and IRE1.[21] HCV induced the phosphorylation of PERK and its downstream effector eIF2α, which in turn led to the increased expression of ATF4, CHOP/GADD153, and the protein chaperon GRP78 (Fig. 5A). We then examined the effect of HCV on IRE1, which, on its activation, induces the splicing of the *xbp1* mRNA to stimulate the expression of UPR target genes.[21] Splicing of *xbp1* mRNA was assayed by RT-PCR: the unspliced RNA generates a 442-bp product that can be digested by the restriction enzyme Pst1, whereas the spliced RNA generates a 416-bp Pst1-resistant product.[22] The spliced *xbp1* RNA was easily detectable in cells transfected with the JFH1 RNA but not in cells transfected with the GND RNA or in untransfected cells (Fig. 5B). As a positive control, we treated naïve Huh7.5 cells with DTT, a chemical that causes protein misfolding and ER stress.[22] As expected, this treatment induced the splicing of *xbp1* mRNA in Huh7.5 cells (Fig. 5B).

We also investigated the effect of HCV on the ATF6 signaling pathway. ATF6 is cleaved from the 90-kDa inactive form to a 50-kDa active fragment on ER stress induction. A low level of activated ATF6 was detected in cells that were transfected with the HCV JFH1 RNA but not in cells that were transfected with the replication defective GND RNA (Fig. 5C). Huh7.5 cells treated with DTT served as the positive control, because they showed efficient ATF6 cleavage (Fig. 5C).

Induction of Autophagosomes by HCV via ER Stress. The results shown in Fig. 5 indicated that HCV could induce ER stress to activate all three arms of the UPR. Next, we examined whether ER stress could induce autophagy in Huh7.5 cells. Treatment of cells with the ER stress inducer Tg or DTT induced the formation of LC3-II (Fig. 6A), the colocalization of GFP-LC3 puncta with LysoTracker-red (Fig. 6B), and an increase of overall and BAF-sensitive protein degradation rate (Fig. 6C).

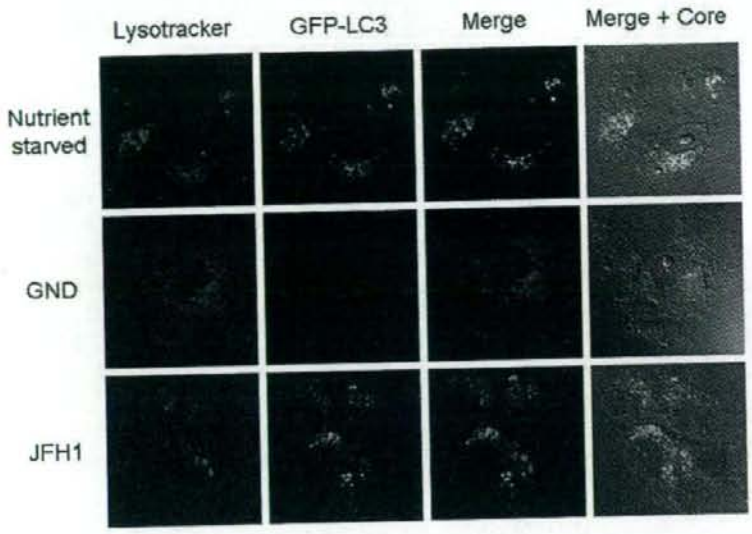

Fig. 4. Inefficient maturation of autophagic vacuoles induced by HCV. Cells were nutrient starved (top panels) or transfected with the HCV GND RNA (middle panels) or JFH1 RNA (bottom panels). The Merge panels combine LysoTracker (red) and GFP-LC3 (green) signals, whereas the Merge+Core panels combine LysoTracker (red), GFP-LC3, the HCV core protein staining (blue), and phase-contrast micrograph. The HCV core protein was stained with the rabbit anti-core primary antibody and the Alexa Fluor 405-conjugated goat anti-rabbit secondary antibody (Invitrogen, Carlsbad, CA).

These observations indicated that ER stress could induce autophagy in Huh7.5 cells. To test whether HCV JFH1 indeed induced the accumulation of autophagosomes via the induction of ER stress, we treated HCV JFH1 cells with siRNAs directed against PERK, IRE1, and ATF6. Two different siRNAs directed against PERK reduced significantly the PERK protein level in HCV JFH1 cells (Fig. 7A). In contrast, a control siRNA had no effect on the total PERK protein level. The suppression of PERK function by the siRNAs was confirmed by the observation that the phosphorylation of eIF2α, a substrate of PERK, was reduced by PERK siRNAs (Fig. 7A). Neither the control siRNA nor the PERK-specific siRNAs affected the total eIF2α protein level in HCV JFH1 cells. We then examined whether the suppression of PERK expression by siRNA would affect the lipidation of LC3 by HCV. Although the LC3-II level was not affected by the control siRNA, it was significantly reduced by the PERK siRNAs (Fig. 7A). These results indicated a critical role of PERK in the autophagic response induced by HCV.

In the IRE1 knockdown experiment, the siRNA directed against IRE1 but not the control siRNA significantly reduced the IRE1 protein level (Fig. 7B). The IRE1 siRNA but not the control siRNA also reduced the LC3-II protein level. Similarly, in the ATF6 knockdown experiment, the siRNA directed against ATF6 significantly reduced uncleaved and cleaved ATF6 protein levels and also the LC3-II protein level (Fig. 7C).

As a control, we also analyzed the effects of PERK, IRE1, and ATF6 siRNAs on LC3 in naïve Huh7.5 cells. None of these siRNAs had any effect on LC3 (Supplementary Fig. 3). These results indicated that

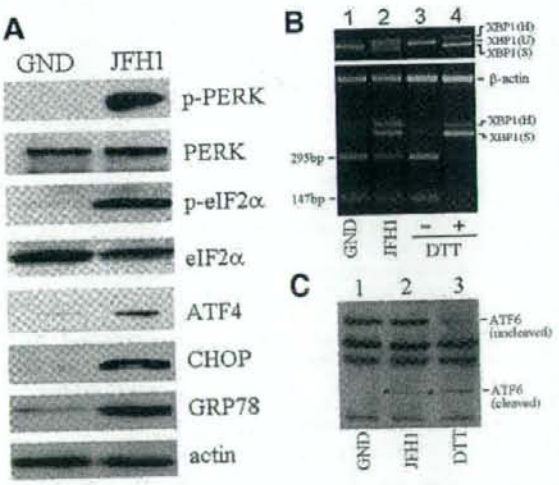

Fig. 5. Activation of the unfolded protein response by HCV JFH1. (A) Activation of the PERK signaling pathway. Huh7.5 cells electroporated with JFH1 or JFH1/GND RNA were lysed 3 days posttransfection for western blot analysis of the proteins indicated. p-PERK and p-eIF2α indicated the phosphorylated PERK and eIF2α, respectively. (B) Activation of the IRE1-XBP1 signaling pathway. Total cellular RNA was analyzed for XBP1 RNA by semi-quantitative RT-PCR. Upper panel, undigested RT-PCR products; lower panel, Pst1-digested PCR products. XPB1 (U) and (S) represent DNA fragments derived from unspliced and spliced XBP1 RNA, respectively. XBP1 (H) represents the hybrid DNA derived from XBP1 (U) and XBP1 (S). The β-actin RNA was also analyzed to serve as an internal control. Digestion of XBP1 (U) by Pst1 would generate the 295-bp and the 147-bp DNA fragments. Lane 1, JFH1/GND RNA transfected cells; lane 2, JFH1 RNA transfected cells; lane 3, naïve Huh7.5 cells without DTT treatment to serve as a negative control; and lane 4, Huh7.5 cells with DTT treatment to serve as the positive control. (C) Activation of ATF6. Huh7.5 cells transfected with JFH1/GND (lane 1) or JFH1 (lane 2) RNA or treated with DTT (lane 3) were lysed for ATF6 analysis by western blot. The locations of uncleaved and cleaved ATF6 are indicated. Asterisks highlight the cleaved ATF6 protein band in JFH1 cells.

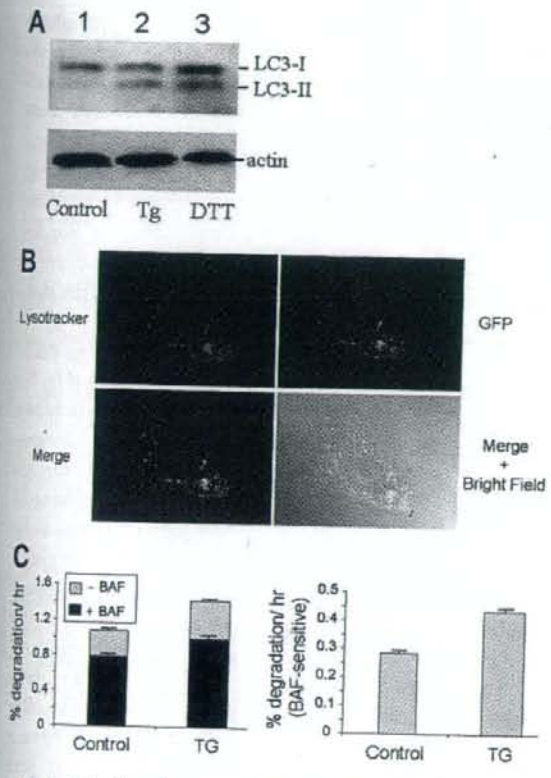

Fig. 6. Induction of autophagy by ER stress in Huh7.5 cells. (A) Induction of LC3 lipidation by ER stress inducers Tg and DTT. Huh7.5 cells without treatment (lane 1), with 300 nM Tg treatment for 16 hours (lane 2), or with 5 mM DTT treatment for 30 minutes (lane 3) were analyzed by western blotting for LC3 and actin. (B) Confocal microscopy of autophagic vacuoles. Stable Huh7.5 cells that expressed GFP-LC3 were stained with LysoTracker-red for 3 hours and further treated with DTT for 20 minutes. (C) Long-lived protein degradation assay. Cells with or without Tg treatment for 16 hours were analyzed for protein degradation as described in the Fig. 3 legend. The overall protein degradation rates in the absence (gray bar) or in the presence (black bar) of BAF are shown in the top panel, and the BAF-sensitive protein degradation rates are highlighted in the bottom panel.

PERK, IRE1, and ATF6 pathways were also important for the lipidation of LC3 induced by HCV. The role of ER stress in LC3 lipidation was further confirmed by the treatment of cells with the chemical chaperon 4-phenylbutyric acid, which reduced the LC3-II level in HCV cells (Supplementary Fig. 4).

Positive Effect of ER Stress and Autophagic Pathway in HCV RNA Replication. To investigate the possible effect of ER stress and the autophagic pathway on HCV RNA replication, cells treated with control siRNA or siRNA directed against PERK, IRE1, or ATF6 were analyzed for HCV RNA levels by qRT-PCR. The siRNAs directed against PERK, IRE1, and ATF6 reduced the HCV RNA level by approximately 80%, 98%, and 80%, respectively, as compared with HCV RNA levels in cells treated with the control siRNA (Fig. 8A). These results indicated that ER stress and likely also autophagosomes played a positive role in HCV RNA replication. To confirm the role of the autophagosomes in HCV RNA replication, we conducted additional knockdown experiments using siRNAs directed against LC3 and Atg7. The LC3 siRNA reduced both LC3-I and LC3-II protein levels, whereas the Atg7 siRNA reduced the Atg7 protein level and the LC3-II level (Fig. 8B). The LC3 siRNA and the Atg7 siRNA also reduced the HCV RNA level by approximately 70% and 55% in JFH1 cells (Fig. 8A), confirming a positive role of autophagosomes or the pathway leading to its accumulation in HCV RNA replication.

Discussion

Several viruses have been shown to induce autophagy. [23] Our results demonstrated that HCV also induces the accumulation of autophagosomes in its host cells (Figs. 1 and 2). The ability of HCV to induce autophagosomes is not limited to the genotype 2a

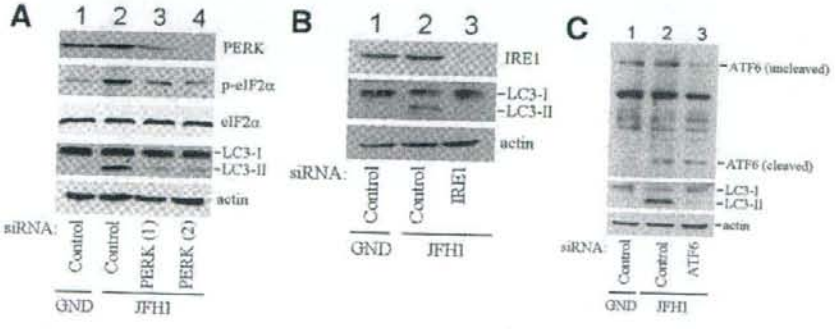

Fig. 7. Induction of LC3 lipidation by HCV via the unfolded protein response. Huh7.5 cells were electroporated with JFH1/GND RNA (lane 1) or JFH1 RNA followed by transfection with a control siRNA (lanes 1 and 2) or siRNAs directed against PERK (A; lanes 3 and 4), IRE1 (B; lane 3), or ATF6 (C; lane 3). Cells were then lysed for western blot analysis.

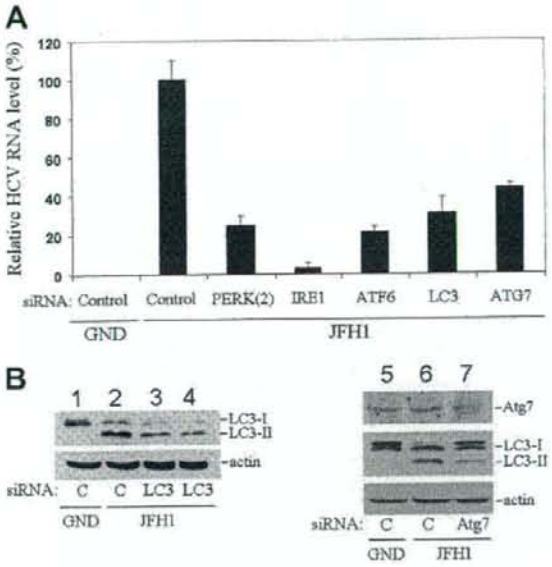

Fig. 8. Effects of ER stress and LC3 on HCV RNA replication. (A) Quantification of HCV RNA. Huh7.5 cells electroporated with either GND RNA or JFH1 RNA were further transfected using the siRNAs indicated under the chart for 48 hours. Total cellular RNA was then isolated for qRT-PCR analysis. JFH1 cells transfected with the control siRNA were arbitrarily defined as 100%. The results represent the average of at least three independent experiments. The PERK(2) siRNA, which was more efficient in suppressing the expression of PERK, was used for the analysis. (B) Western blot analysis of LC3 and Atg7. Cells in a 10-cm dish transfected by the GND RNA (lanes 1 and 5), JFH1 RNA (lanes 2-4 and 6-7) were further transfected with the control (C) siRNA (lanes 1, 2, 5, and 6), 4.7 μg LC3 siRNA (lane 3), 9.5 μg LC3 siRNA (lane 4), or 9.5 μg Atg7 siRNA (lane 7).

HCV JFH1 strain, as this induction was also observed in Huh7 cells harboring the genotype 1b Con1 virus subgenomic RNA replicon (Fig. 2B). While this manuscript was in preparation, it was also reported that the HCV genotype 1a virus could induce the accumulation of autophagic vacuoles.[24] Thus, the ability of HCV to induce autophagosomes is shared by HCV strains across different genotypes. Although HCV JFH1 was able to induce autophagosomes, however, it was not able to enhance autophagic protein degradation (Fig. 3). This lack of enhancement of autophagic degradation by HCV is apparently attributable to the inefficient fusion between autophagosomes and lysosomes (Fig. 4).

How viruses induce autophagy has remained largely unclear. Our results demonstrated that HCV induced the accumulation of autophagosomes via the induction of ER stress (Figs. 5 and 6). This induction of autophagosomes involved all three arms of the UPR (Fig. 7), as the suppression of any of these three pathways suppressed the lipidation of LC3, an essential step for the formation of autophagosomes. This observation is interesting, because it indicated that the target genes activated by these different signaling pathways must work in concert with one another to induce autophagy. ER stress can enhance autophagy in Huh7.5 cells (Fig. 6). However, the autophagy activated by HCV is incomplete, because autophagic degradation is not increased (Fig. 3). It is likely that HCV factors or other signaling pathways activated by HCV perturb the maturation of autophagic vacuoles (Fig. 4).

The suppression of any of the three signaling pathways of UPR decreased HCV RNA replication (Fig. 8). This is at least partially through the suppression of the autophagic response, because suppressing the expression of Atg7 and LC3, two proteins necessary for autophagosome formation, also led to a reduced level of HCV RNA replication (Fig. 8). Thus, our results indicated that ER stress and the autophagic pathway play a positive role in HCV replication. It does not appear likely that HCV uses autophagosomes as sites for virion morphogenesis, because the HCV core protein and autophagosomes do not colocalize (Fig. 1B). The replication complexes of several positive RNA viruses localize to autophagosomes,[25-28] but it remains to be determined whether the HCV RNA replication complex also resides on autophagosomes or on membranes derived from autophagosomes.

In conclusion, our studies demonstrated that HCV induced ER stress and an incomplete autophagic response. The persistent induction of ER stress and the incomplete activation of autophagy likely play an important role in HCV pathogenesis. Our results also suggest that the many viruses that are capable of inducing ER stress have the potential to induce an autophagic response. The outcome of this response, however, would likely vary for individual viruses, because autophagy is a cellular mechanism to clear viral infection, whereas, conversely, viruses such as HCV appear to have used this cellular response to enhance their own replication.

Acknowledgment: The authors thank Dr. Amy Lee for helpful discussions on ER stress during the course of our studies and Dr. David Ann for helpful suggestions on autophagy studies and for critical reading of this manuscript. We also thank Dr. Charles Rice for providing us with the Huh7.5 cells, Michelle McVeigh at the USC Research Center for Liver Diseases for help with confocal microscopy, and Sandra Huling of the SFVAMC/NCIRE Microscopy Core for electron microscopy.

References

1. Levine B, Kroemer G. Autophagy in the pathogenesis of disease. Cell 2008;132:27-42.
2. Kirkegaard K, Taylor MP, Jackson WT. Cellular autophagy: surrender, avoidance and subversion by microorganisms. Nat Rev Microbiol 2004;2: 301-314.
3. Moradpour D, Penin F, Rice CM. Replication of hepatitis C virus. Nat Rev Microbiol 2007;5:453-463.
4. Wakita T, Pietschmann T, Kato T, Date T, Miyamoto M, Zhao Z, et al. Production of infectious hepatitis C virus in tissue culture from a cloned viral genome. Nat Med 2005;11:791-796.
5. Lindenbach BD, Evans MJ, Syder AJ, Wolk B, Tellinghuisen TL, Liu CC, et al. Complete replication of hepatitis C virus in cell culture. Science 2005;309:623-626.
6. Zhong J, Gastaminza P, Cheng G, Kapadia S, Kato T, Burton DR, et al. Robust hepatitis C virus infection in vitro. Proc Natl Acad Sci U S A 2005;102:9294-9299.
7. Cai Z, Zhang C, Chang KS, Jiang J, Ahn BC, Wakita T, et al. Robust production of infectious hepatitis C virus (HCV) from stably HCV cDNA-transfected human hepatoma cells. J Virol 2005;79:13963-13973.
8. Kabeya Y, Mizushima N, Ueno T, Yamamoto A, Kirisako T, Noda T, et al. LC3, a mammalian homologue of yeast Apg8p, is localized in autophagosome membranes after processing. EMBO J 2000;19:5720-5728.
9. Kato T, Date T, Miyamoto M, Furusaka A, Tokushige K, Mizokami M, et al. Efficient replication of the genotype 2a hepatitis C virus subgenomic replicon. Gastroenterology 2003;125:1808-1817.
10. Choi J, Lee KJ, Zheng Y, Yamaga AK, Lai MM, Ou JH. Reactive oxygen species suppress hepatitis C virus RNA replication in human hepatoma cells. HEPATOLOGY 2004;39:81-89.
11. Shang J, Gao N, Kaufman RJ, Ron D, Harding HP, Lehrman MA. Translation attenuation by PERK balances ER glycoprotein synthesis with lipid-linked oligosaccharide flux. J Cell Biol 2007;176:605-616.
12. Zhu JH, Horbinski C, Guo F, Watkins S, Uchiyama Y, Chu CT. Regulation of autophagy by extracellular signal-regulated protein kinases during 1-methyl-4-phenylpyridinium-induced cell death. Am J Pathol 2007;170: 75-86.
13. Yamamoto A, Tagawa Y, Yoshimori T, Moriyama Y, Masaki R, Tashiro Y. Bafilomycin A1 prevents maturation of autophagic vacuoles by inhibiting fusion between autophagosomes and lysosomes in rat hepatoma cell line, H-4-II-E cells. Cell Struct Funct 1998;23:33-42.
14. Bjorkoy G, Lamark T, Brech A, Outzen H, Perander M, Overvatn A, et al. p62/SQSTM1 forms protein aggregates degraded by autophagy and has a protective effect on huntingtin-induced cell death. J Cell Biol 2005;171: 603-614.
15. Benali-Furet NL, Chami M, Houel L, De Giorgi F, Vernejoul F, Lagorce D, et al. Hepatitis C virus core triggers apoptosis in liver cells by inducing ER stress and ER calcium depletion. Oncogene 2005;24:4921-4933.
16. Chan SW, Egan PA. Hepatitis C virus envelope proteins regulate CHOP via induction of the unfolded protein response. FASEB J 2005;19:1510-1512.
17. Liberman E, Fong YL, Selby MJ, Choo QL, Cousens L, Houghton M, et al. Activation of the grp78 and grp94 promoters by hepatitis C virus E2 envelope protein. J Virol 1999;73:3718-3722.
18. Tardif KD, Mori K, Kaufman RJ, Siddiqui A. Hepatitis C virus suppresses the IRE1-XBP1 pathway of the unfolded protein response. J Biol Chem 2004;279:17158-17164.
19. Ogata M, Hino S, Saito A, Morikawa K, Kondo S, Kanemoto S, et al. Autophagy is activated for cell survival after endoplasmic reticulum stress. Mol Cell Biol 2006;26:9220-9231.
20. Kouroku Y, Fujita E, Tanida I, Ueno T, Isoai A, Kumagai H, et al. ER stress (PERK/eIF2alpha phosphorylation) mediates the polyglutamine-induced LC3 conversion, an essential step for autophagy formation. Cell Death Differ 2007;14:230-239.
21. Ron D, Walter P. Signal integration in the endoplasmic reticulum unfolded protein response. Nat Rev Mol Cell Biol 2007;8:519-529.
22. Yoshida H, Oku M, Suzuki M, Mori K. pXBP1(U) encoded in XBP1 pre-mRNA negatively regulates unfolded protein response activator pXBP1(S) in mammalian ER stress response. J Cell Biol 2006;172:565-575.
23. Lee HK, Iwasaki A. Autophagy and antiviral immunity. Curr Opin Immunol 2008.
24. Ait-Goughoulte M, Kanda T, Meyer K, Ryerse JS, Ray RB, Ray R. Hepatitis C virus genotype 1a growth and induction of autophagy. J Virol 2008;82:2241-2249.
25. Jackson WT, Giddings TH, Jr., Taylor MP, Mulinyawe S, Rabinovitch M, Kopito RR, et al. Subversion of cellular autophagosomal machinery by RNA viruses. PLoS Biol 2005;3:e156.
26. Prentice E, Jerome WG, Yoshimori T, Mizushima N, Denison MR. Coronavirus replication complex formation utilizes components of cellular autophagy. J Biol Chem 2004;279:10136-10141.
27. Pedersen KW, van der Meer Y, Roos N, Snijder EJ. Open reading frame 1a-encoded subunits of the arterivirus replicase induce endoplasmic reticulum-derived double-membrane vesicles which carry the viral replication complex. J Virol 1999;73:2016-2026.
28. Goldsmith CS, Tatti KM, Ksiazek TG, Rollin PE, Comer JA, Lee WW, et al. Ultrastructural characterization of SARS coronavirus. Emerg Infect Dis 2004;10:320-326.

JOURNAL OF VIROLOGY, Oct. 2008, p. 9639–9646 Vol. 82, No. 19
0022-538X/08/$08.00+0 doi:10.1128/JVI.00351-08

The DNA Damage Sensors Ataxia-Telangiectasia Mutated Kinase and Checkpoint Kinase 2 Are Required for Hepatitis C Virus RNA Replication▽

Yasuo Ariumi,[1] Misao Kuroki,[1] Hiromichi Dansako,[1] Ken-Ichi Abe,[1] Masanori Ikeda,[1] Takaji Wakita,[2] and Nobuyuki Kato[1]*

Department of Molecular Biology, Okayama University Graduate School of Medicine, Dentistry, and Pharmaceutical Sciences, 2-5-1, Shikata-cho, Okayama 700-8558, Japan,[1] and Department of Virology II, National Institute of Infectious Diseases, 1-23-1 Toyama, Shinjuku-ku, Tokyo 162-8640, Japan[2]

Received 18 February 2008/Accepted 18 July 2008

Cellular responses to DNA damage are crucial for maintaining genome integrity, virus infection, and preventing the development of cancer. Hepatitis C virus (HCV) infection and the expression of the HCV nonstructural protein NS3 and core protein have been proposed as factors involved in the induction of double-stranded DNA breaks and enhancement of the mutation frequency of cellular genes. Since DNA damage sensors, such as the ataxia-telangiectasia mutated kinase (ATM), ATM- and Rad3-related kinase (ATR), poly(ADP-ribose) polymerase 1 (PARP-1), and checkpoint kinase 2 (Chk2), play central roles in the response to genotoxic stress, we hypothesized that these sensors might affect HCV replication. To test this hypothesis, we examined the level of HCV RNA in HuH-7-derived cells stably expressing short hairpin RNA targeted to ATM, ATR, PARP-1, or Chk2. Consequently, we found that replication of both genome-length HCV RNA (HCV-O, genotype 1b) and the subgenomic replicon RNA were notably suppressed in ATM- or Chk2-knockdown cells. In addition, the RNA replication of HCV-JFH1 (genotype 2a) and the release of core protein into the culture supernatants were suppressed in these knockdown cells after inoculation of the cell culture-generated HCV. Consistent with these observations, ATM kinase inhibitor could suppress the HCV RNA replication. Furthermore, we observed that HCV NS3-NS4A interacted with ATM and that HCV NS5B interacted with both ATM and Chk2. Taken together, these results suggest that the ATM signaling pathway is critical for HCV RNA replication and may represent a novel target for the clinical treatment of patients with chronic hepatitis C.

Hepatitis C virus (HCV) infection frequently causes chronic hepatitis, which progresses to liver cirrhosis and hepatocellular carcinoma. HCV infection has now become a serious health problem, with at least 170 million people currently infected worldwide (28). HCV is an enveloped virus with a positive single-stranded 9.6-kb RNA genome, which encodes a large polyprotein precursor of approximately 3,000 amino acid residues. This polyprotein is cleaved by a combination of the host and viral proteases into at least 10 proteins in the following order: core, envelope 1 (E1), E2, p7, nonstructural 2 (NS2), NS3, NS4A, NS4B, NS5A, and NS5B (12, 13, 27).

Studies have shown that various viruses with distinct replication strategies—including the DNA viruses Epstein-Barr virus, herpes simplex virus 1, adenovirus, and simian virus 40 and the retrovirus human immunodeficiency virus type 1 (HIV-1)—can activate DNA damage response pathways and utilize these damage responses to facilitate their own viral reproduction and promote the survival of infected cells (2, 16, 17). In the case of HCV, it has been proposed that HCV infection causes double-stranded DNA (dsDNA) breaks and enhances the mutation frequency of cellular genes and that these effects are mediated by nitric oxide (18, 19). In addition, the HCV core, E1, and NS3 proteins have been suggested to be potent reactive oxygen species inducers, leading to DNA damage (19). Furthermore, we previously demonstrated that HCV NS5B-expressing PH5CH8 immortalized human hepatocyte cells were susceptible to DNA damage in the form of dsDNA breaks (23). Thus, HCV seems to be associated with the dsDNA damage response pathways.

Since the DNA damage sensors, such as ataxia-telangiectasia mutated kinase (ATM), ATM- and Rad3-related kinase (ATR), poly(ADP-ribose) polymerase 1 (PARP-1), and checkpoint kinase 2 (Chk2; a direct downstream target of ATM), play central roles in response to genotoxic stress (10), we hypothesized that these sensors might affect HCV replication.

To investigate the possible involvement of these cellular factors in HCV replication, we examined the level of HCV RNA in cells rendered defective for DNA damage sensors by RNA interference or by pharmacological inhibition.

MATERIALS AND METHODS

Cell culture. 293FT cells were cultured in Dulbecco's modified Eagle's medium (DMEM; Invitrogen, Carlsbad, CA) supplemented with 10% fetal bovine serum (FBS). The HuH-7-derived O cells harboring a replicative genome-length HCV RNA and the HuH-7-derived sO cells harboring the subgenomic replicon RNA of HCV-O were cultured in DMEM with 10% FBS and G418 (300 μg/ml geneticin; Invitrogen) as described previously (11, 14). Oc and sOc cells, which were created by eliminating HCV RNA from O cells and sO cells by interferon (IFN) treatment (11, 14), respectively, were also cultured in DMEM with 10% FBS.

RNA interference. Oligonucleotides with the following sense and antisense sequences were used for the cloning of short hairpin RNA (shRNA)-encoding se-

* Corresponding author. Mailing address: Department of Molecular Biology, Okayama University Graduate School of Medicine, Dentistry, and Pharmaceutical Sciences, 2-5-1, Shikata-cho, Okayama 700-8558, Japan. Phone: 81 86 235 7385. Fax: 81 86 235 7392. E-mail: nkato@md.okayama-u.ac.jp.

▽ Published ahead of print on 30 July 2008.

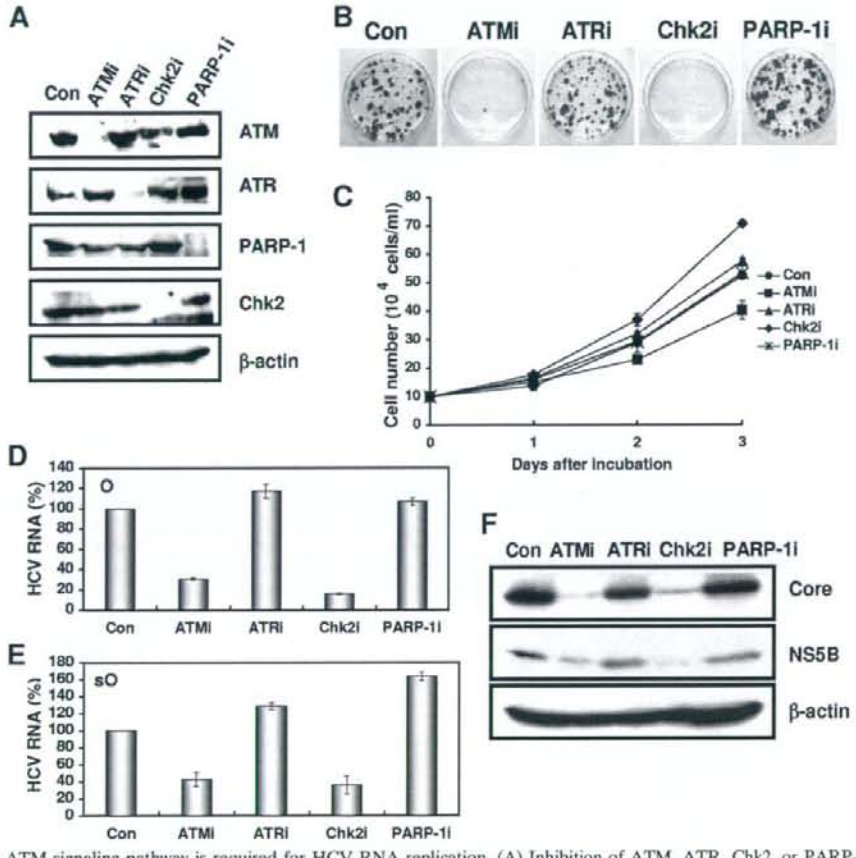

FIG. 1. The ATM signaling pathway is required for HCV RNA replication. (A) Inhibition of ATM, ATR, Chk2, or PARP-1 expression by shRNA-producing lentiviral vectors. The results of the Western blot analysis of cellular lysates with anti-ATM, anti-ATR, anti-Chk2, anti-PARP-1, or anti-β-actin antibody in Oc cells expressing shRNA targeted to ATM (ATMi), ATR (ATRi), Chk2 (Chk2i), or PARP-1 (PARP-1i) as well as in Oc cells transduced with a control lentiviral vector (Con) are shown. (B) ECF in ATM-, ATR-, Chk2-, or PARP-1-knockdown cells. In vitro transcribed ON/C-5B K1609E RNA (2 μg) was transfected into the ATM-, ATR-, Chk2, or PARP-1-knockdown Oc cells or the Oc cells transduced with a control lentiviral vector (Con). G418-resistant colonies were stained with Coomassie brilliant blue at 3 weeks after electroporation of RNA. Experiments were done in duplicate, and a representative result is shown. (C) The cell growth curve of ATM (ATMi), ATR (ATRi), Chk2 (Chk2i), or PARP-1 (PARP-1i)-knockdown Oc cells or the Oc cells transduced with a control lentiviral vector (Con). Results from three independent experiments are shown. (D) The level of genome-length HCV-O RNA was monitored by real-time LightCycler PCR (Roche). Experiments were done in triplicate, and columns represent the mean percentage of HCV RNA. (E) The level of subgenomic replicon (sO cells) RNA was monitored by real-time LightCycler PCR. Results from three independent experiments are shown as described in panel D. (F) The HCV core or NS5B protein expression level in ATM-, ATR-, Chk2-, or PARP-1-knockdown cells. The results of Western blot analysis of cellular lysates with anti-HCV core protein, anti-HCV NS5B, or anti-β-actin antibody in O cells expressing shRNA targeted to ATM (ATMi), ATR (ATRi), Chk2 (Chk2i), or PARP-1 (PARP-1i) as well as in O cells transduced with a control lentiviral vector (Con) are shown.

quences targeted to Chk2 in lentiviral vector: 5′-GATCCCCGGGGGAGAGCTGTT TGACATTCAAGAGATGTCAAACAGCTCTCCCCCTTTTTGGAAA-3′ (sense) and 5′-AGCTTTTCCAAAAAGGGGGAGAGCTGTTTGACATCTCTTGAATGT CAAACAGCTCTCCCCCGGG-3′ (antisense). The oligonucleotides above were annealed and subcloned into the BglII-HindIII site, downstream from an RNA polymerase III promoter of pSUPER (5), generating pSUPER-Chk2i. To construct pLV-Chk2i, the BamHI-SalI fragments of the pSUPER-Chk2i were subcloned into the BamHI-SalI site of pRDI292, an HIV-1-derived self-inactivating lentiviral vector containing a puromycin resistance marker allowing for the selection of transduced cells (4). pLV-ATMi, pLV-ATRi, and pLV-PARP-1i were constructed as described previously (1).

Lentiviral vector production. The vesicular stomatitis virus G protein (VSV-G)-pseudotyped HIV-1-based vector system has been described previously (24). The lentiviral vector particles were produced by transient transfection of the second-generation packaging construct pCMV-ΔR8.91 (30) and the VSV-G envelope plasmid pMDG2 as well as the lentiviral vector into 293FT cells with FuGene6 (Roche Diagnostics, Mannheim, Germany).

Quantitative reverse transcription-PCR analysis. Quantitative reverse transcription-PCR analysis for HCV RNA was performed by real-time LightCycler PCR as described previously (11).

Western blot analysis. Cells were lysed in buffer containing 50 mM Tris-HCl (pH 8.0), 150 mM NaCl, 4 mM EDTA, 1% Nonidet P-40, 0.1% sodium dodecyl sulfate (SDS), 1 mM dithiothreitol, and 1 mM phenylmethylsulfonyl fluoride. Supernatants from these lysates were subjected to SDS-polyacrylamide gel electrophoresis, followed by immunoblotting analysis using anti-ATM (2C1; GTX70103 [GeneTex, San Antonio, TX]), anti-ATR (GTX70133; GeneTex), anti-Chk2 (NT; ProSci, Poway, CA), anti-Chk2 (DCS-273; Medical and Biological Laboratories, Nagoya, Japan), anti-phospho-Chk2 (Thr68) (Cell Signaling,

Danvers, MA), anti-PARP-1 (C-2-10; Calbiochem, Merck Biosciences, Darmstadt, Germany), anti-hemagglutinin (HA) (HA-7; Sigma, St. Louis, MO), anti-core protein (CP-9 and CP-11; Institute of Immunology, Tokyo, Japan), anti-NS3 and anti-NS5B (no. 14; a generous gift from M. Kohara, the Tokyo Metropolitan Institute of Medical Science, Japan), anti-NS5A (no. 8926; a generous gift from A. Takamizawa, The Research Foundation for Microbial Diseases of Osaka University, Japan), and anti-β-actin (Sigma) Antibodies.

Immunofluorescence and confocal microscopic analysis. Cells were fixed in 3.5% formaldehyde in phosphate-buffered saline (PBS) and permeabilized in 0.1% NP-40 in PBS at room temperature. Cells were incubated with anti-ATM antibody (5C2; GTX70107 [GeneTex] or PM026 [MBL]), anti-HA antibody (3F10), anti-NS5B antibody and/or anti-NS3 antibody at a 1:300 dilution in PBS containing 3% bovine serum albumin at 37°C for 30 min. Cells were then stained with fluorescein isothiocyanate (FITC)-conjugated anti-rabbit antibody (Jackson ImmunoResearch, West Grove, PA) or anti-Cy3-conjugated anti-mouse antibody (Jackson ImmunoResearch) at a 1:300 dilution in PBS containing bovine serum albumin at 37°C for 30 min. Following extensive washing in PBS, cells were mounted on slides using a mounting medium of 90% glycerin–10% PBS with 0.01% *p*-phenylenediamine added to reduce fading. Samples were viewed under a confocal laser-scanning microscope (LSM510; Zeiss, Jena, Germany).

Immunoprecipitation. Cells were lysed in buffer containing 10 mM Tris-HCl (pH 8.0), 150 mM NaCl, 4 mM EDTA, 0.5% NP-40, 10 mM NaF, 1 mM dithiothreitol, and 1 mM phenylmethylsulfonyl fluoride. Lysates were precleared with 30 μl of protein G-Sepharose (GE Healthcare Biosciences, Uppsala, Sweden). Precleared supernatants were incubated with 5 μg of anti-HA antibody (3F10; Roche), 10 μl of anti-NS5B antibody, 5 μg of anti-Chk2 antibody (DCS-273; MBL), 5 μg of anti-FLAG antibody (M2; Sigma), or 5 μg of anti-ATM antibody (2C1) (GTX70103; GeneTex) at 4°C for 1 h. Following absorption of the precipitates on 30 μl of protein G-Sepharose resin for 1 h, the resin was washed four times with 700 μl of lysis buffer. Proteins were eluted by boiling the resin for 5 min in 2× Laemmli sample buffer. The proteins were then subjected to SDS-polyacrylamide gel electrophoresis, followed by immunoblotting analysis using anti-ATM, anti-Chk2, anti-HCV core protein (CP-9 and CP-11 mixture), anti-NS5A, anti-NS5B, anti-HA (HA-7; Sigma), or anti-NS3 antibody.

RESULTS

ATM and Chk2 are required for HCV RNA replication. To determine the potential role of DNA damage sensors in HCV replication, we first used lentiviral vector-mediated RNA interference to stably knockdown ATM, ATR, PARP-1 (1), or Chk2 in the following human hepatoma HuH-7-derived cell lines: O cells harboring a replicative genome-length HCV RNA (HCV-O, genotype 1b) (11), Oc cells derived from O cells (created by eliminating genome-length HCV RNA from O cells by IFN treatment) (11), sO cells harboring the subgenomic replicon of HCV-O (14), or RSc cells that cell culture-generated HCV (HCVcc) (JFH1, genotype 2a) (29) could infect and effectively replicate (3). To express shRNAs targeted to ATM, ATR, PARP-1 (1), or Chk2, we used a VSV-G-pseudotyped HIV-1-based vector system (24). We used puromycin-resistant pooled cells 10 days after the lentiviral transduction in all experiments. Western blot analysis of the lysates demonstrated very effective knockdown of ATM, ATR, Chk2, and PARP-1 in Oc cells (Fig. 1A). The effective knockdown of ATM, ATR, Chk2, or PARP-1 in O cells or sO cells was also confirmed by Western blot analysis (data not shown). In this context, the efficiency of colony formation (ECF) in ATM- or Chk2-, but not ATR- or PARP-1-, knockdown Oc cells transfected with the genome-length HCV-O RNA with an adapted mutation at amino acid position 1609 in the NS3 helicase region (ON/C-5B K1609E RNA) (11) was notably reduced compared with the control cells (Fig. 1B) even though Chk2-knockdown cells had a slightly faster growth rate than the control cells (Fig. 1C), suggesting that both ATM and Chk2 are crucial for HCV RNA replication. To further confirm this

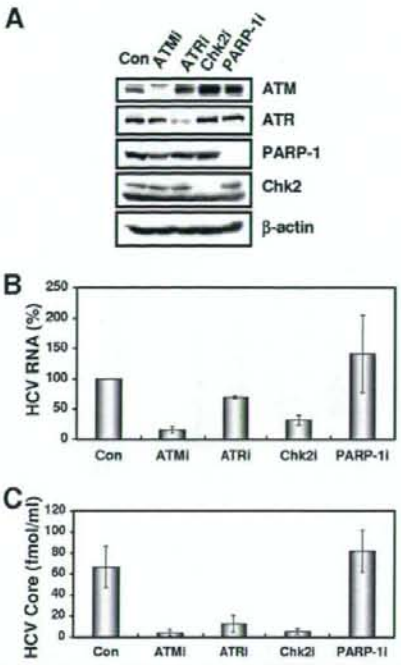

FIG. 2. ATM affects HCV infection. (A) Inhibition of ATM, ATR, Chk2, or PARP-1 expression by shRNA-producing lentiviral vectors. The results of Western blot analysis of cellular lysates with anti-ATM, anti-ATR, anti-PARP-1, anti-Chk2, or anti-β-actin antibody in RSc cured cells expressing shRNA targeted to ATM (ATMi), ATR (ATRi), Chk2 (Chk2i), or PARP-1 (PARP-1i) as well as in RSc cells transduced with a control lentiviral vector (Con) are shown. (B) The level of genome-length HCV (JFH1) RNA was monitored by real-time LightCycler PCR after inoculation of the HCVcc. Results from three independent experiments are shown as described in the legend of Fig. 1D. (C) The levels of the core protein in the culture supernatants were determined by enzyme-linked immunosorbent assay (Mitsubishi Kagaku Bio-Clinical Laboratories). Experiments were done in triplicate, and columns represent the mean core protein levels.

observation, we quantitatively examined the level of HCV RNA in the O cell- or sO cell-derived knockdown cells. Consequently, we found that replication of both genome-length HCV RNA (HCV-O) and its subgenomic replicon RNA (sO) were notably suppressed in ATM- or Chk2-knockdown cells but not in ATR- or PARP-1-knockdown cells (Fig. 1D and E). Consistent with this finding, the expression levels of core and NS5B proteins were also significantly decreased in the cell lysates of ATM- or Chk2-knockdown O cells (Fig. 1F). We next examined the replication level of HCV-JFH1 in ATM-, ATR-, Chk2-, or PARP-1-knockdown RSc cells (Fig. 2A). The results revealed that RNA replication of HCV-JFH1 and release of core protein into the culture supernatants were suppressed in only ATM- or Chk2-knockdown RSc cells after inoculation with HCVcc (Fig. 2B and C). Interestingly, the release of core protein into the culture supernatant was also significantly suppressed in ATR-knockdown RSc cells, while HCV RNA replication was slightly suppressed in these cells

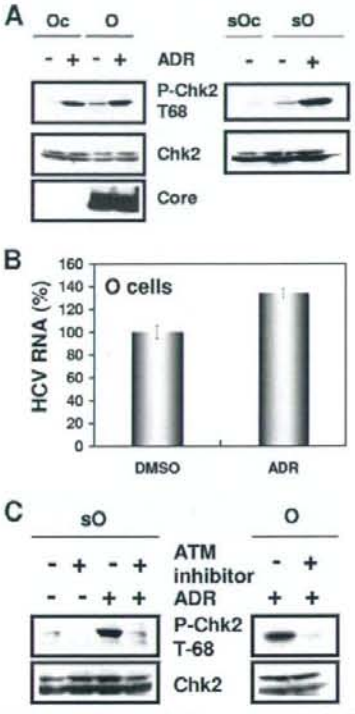

FIG. 3. ATM-dependent DNA damage response in HCV RNA-replicating cells. (A) Stimulation of Chk2 phosphorylation in the HCV RNA-replicating cells. The Oc, O, or sO cells were treated with 100 nM adriamycin (Sigma) for 2 h. The results of Western blot analysis of cellular lysates with anti-phospho-Chk2 (Thr68) (P-Chk2 T68), anti-Chk2, or anti-core protein antibody are shown. (B) Effect of adriamycin on HCV RNA replication. The O cells were treated with 100 nM adriamycin for 24 h. The level of genome-length HCV-O RNA was monitored by real-time LightCycler PCR. Results from three independent experiments are shown as described in the legend of Fig. 1D. DMSO, dimethyl sulfoxide. (C) Effect of ATM kinase inhibitor on Chk2 phosphorylation. The sO or O cells were pretreated with 10 μM ATM kinase inhibitor (KU-55933) (Calbiochem) for 2 h, followed by treatment with 100 nM adriamycin for 2 h. The results of Western blot analysis of cellular lysates with anti-phospho-Chk2 (Thr68) or anti-Chk2 antibody are shown.

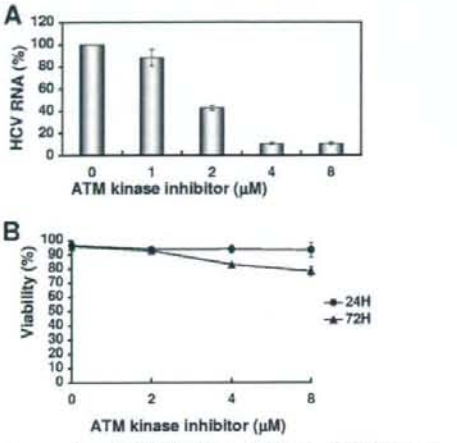

FIG. 4. Suppression of HCV RNA replication by ATM kinase inhibitor. (A) The level of genome-length HCV-O RNA was monitored by real-time LightCycler PCR after treatment with the indicated concentration of ATM kinase inhibitor for 72 h. Results from three independent experiments are shown as described in the legend of Fig. 1D. (B) Cell viabilities after treatment with the indicated concentration of ATM kinase inhibitor for 24 h or 72 h are shown.

(Fig. 2B and C), suggesting that ATR participates in the production of HCV virion.

In contrast, highly efficient knockdown of PARP-1 had no observable effects on the ECF (Fig. 1B), HCV RNA replication (Fig. 1D and E and 2B), or core protein expression in the cell lysate or in the supernatant (Fig. 1F and 2C), suggesting that our finding was not due to a nonspecific event. Thus, we have demonstrated for the first time that DNA damage sensors, ATM and Chk2, are required for HCV RNA replication.

ATM kinase activity in HCV RNA-replicating cells. Although it has been proposed that HCV causes dsDNA breaks (18, 19), little is known about whether HCV activates or inhibits the ATM-dependent damage response pathway. In this regard, it is worth noting that we observed weak but significant Chk2 phosphorylation at threonine 68, the specific marker for ATM activation (20, 21), in the HCV RNA-replicating cells (O and sO cells) but not in the HCV-negative Oc and sOc cells (created by eliminating replicon RNA from sO cells by IFN treatment) (Fig. 3A), suggesting that the persistent HCV RNA replication stimulated the ATM-dependent DNA damage response. Furthermore, a 2-h treatment with 100 nM adriamycin, a dsDNA break inducer, markedly induced Chk2 phosphorylation in Oc, O, and sO cells (Fig. 3A). Importantly, Chk2 phosphorylation was not inhibited even in the HCV RNA-replicating cells (O and sO cells) (Fig. 3A), suggesting that the persistent HCV RNA replication and the HCV proteins are not able to suppress the ATM-dependent DNA damage response. To examine whether such a DNA damage response activates HCV RNA replication, we quantified the level of HCV RNA in the O cells treated with 100 nM adriamycin for 24 h. The results show that HCV RNA replication was increased (approximately 1.3-fold) after treatment with adriamycin (Fig. 3B), suggesting that the DNA damage response activates HCV RNA replication.

Suppression of HCV RNA replication by a small-molecule inhibitor of the ATM kinase. We next examined the effect of a specific small-molecule inhibitor of the ATM kinase (2-morpholin-4-yl-6-thianthren-1-yl-pyran-4-one [KU-55933]) (16) on HCV RNA replication. As expected, the ATM kinase inhibitor effectively inhibited Chk2 phosphorylation after adriamycin treatment in both sO and O cells (Fig. 3C). In this context, the ATM kinase inhibitor could efficiently suppress genome-length HCV RNA replication with an in vitro 50% effective concentration (EC_{50}) of approximately 2 μM at 72 h after treatment with adriamycin (Fig. 4A). Although this ATM kinase inhibitor did not affect cell viability at 24 h after the treatment, there was a slight decrease in the cell viability at 72 h after treatment (Fig. 4B). Thus, this or other ATM kinase inhibitors may be

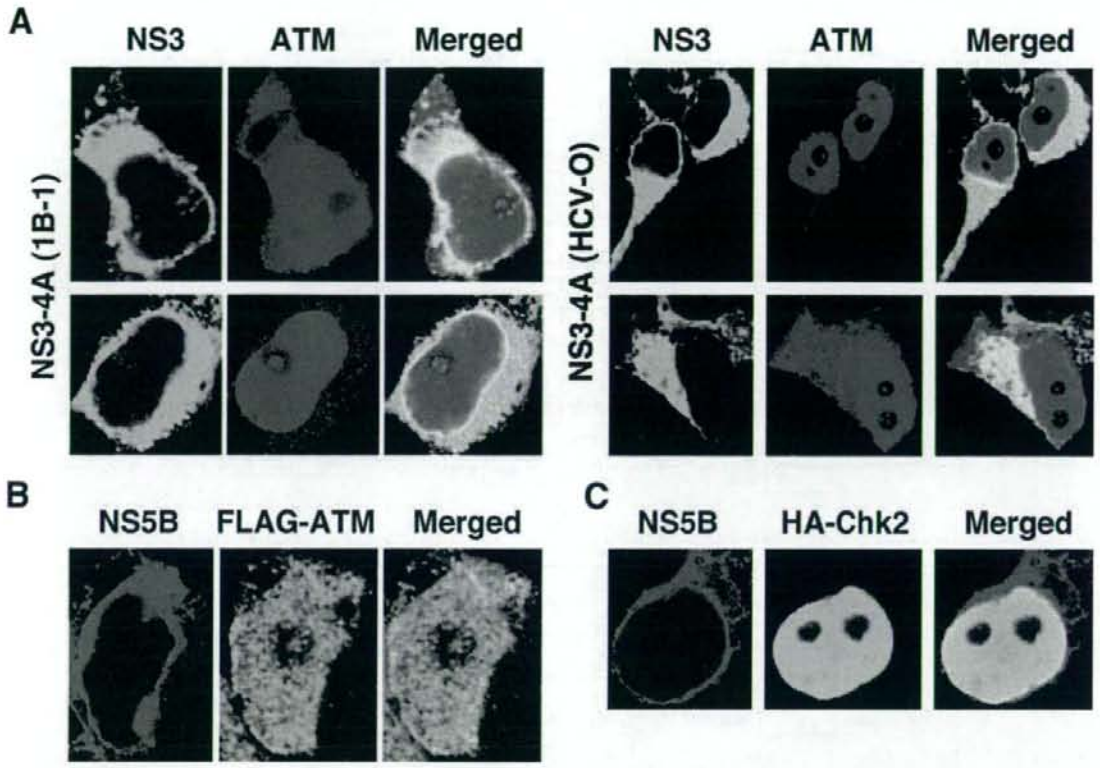

FIG. 5. Subcellular localization of ATM and Chk2 in HCV NS3-4A- or NS5B-expressing cells. (A) ATM partially colocalized with HCV NS3-4A. 293FT cells cotransfected with 300 ng of pCX4bsr/NS3-4A (1B-1) (8) or pCX4bsr/NS3-4A (O) (8) and 300 ng of pcDNA3-FLAG-ATMwt (6) were examined by confocal laser scanning microscopy. Cells were stained with anti-NS3 and anti-ATM (5C2) antibodies and then visualized with FITC (NS3) or Cy3 (ATM). (B) ATM partially colocalized with HCV NS5B. 293FT cells cotransfected with 300 ng of pCX4bsr/NS5B (1B-1) (23) and 300 ng of pcDNA3-FLAG-ATMwt (6). Cells were stained with anti-NS5B (no. 14) and anti-ATM (PM026) antibodies and then visualized with FITC (ATM) or Cy3 (NS5B). (C) Chk2 partially colocalized with HCV NS5B. 293FT cells cotransfected with 300 ng of pCX4bsr/NS5B (1B-1) (23) and 300 ng of pcDNA3-HA-Chk2wt (20, 21). Cells were stained with anti-NS5B and anti-HA (3F10) antibodies and then visualized with FITC (HA-Chk2) or Cy3 (NS5B). Images were visualized using confocal laser scanning microscopy (LSM510; Carl Zeiss). The right panels exhibit two-color overlay images (Merged). Colocalization is shown in yellow.

useful for the clinical treatment of patients with chronic hepatitis C.

Interaction of HCV NS3-4A with ATM. Since HCV NS3 has been proposed to be a viral factor involved in the induction of dsDNA breaks (18, 19), we first examined the subcellular localization of NS3-NS4A ([NS3-4A] 1B-1 or HCV-O strain) and ATM by confocal laser scanning microscopy. In most of the observed cells, ATM partially colocalized with NS3-4A in the perinuclear region and in dispersed points throughout the cytoplasm (Fig. 5A). In particular, we observed prominent colocalization of ATM with NS3-4A in some cells (Fig. 5A). Next, using anti-FLAG and anti-ATM antibodies, we immunoprecipitated lysates from 293FT cells in which FLAG-tagged ATM and either NS3-4A (HCV-O) or NS3 (HCV-O) were overexpressed and then performed immunoblotting analysis using either anti-ATM or anti-NS3 antibody to determine whether ATM binds to NS3-4A or NS3. The results revealed that ATM preferentially bound to NS3-4A over NS3 alone (Fig. 6A). Similarly, we found that ATM bound to NS3-4A using the O cell lysates (Fig. 6B), while HA-tagged Chk2 did not bind to NS3-4A in immunoprecipitation analysis using lysates from 293FT cells in which NS3-4A and HA-tagged Chk2 were overexpressed (Fig. 6C). Although NS3-4A has protease activity, ATM was not cleaved by the NS3-4A protease (Fig. 6D). Taking these results together, we conclude that ATM is able to interact with NS3-4A.

Interaction of HCV NS5B with ATM and Chk2. We next examined the subcellular localization of ATM and/or Chk2 in HCV NS5B-expressing cells by confocal laser scanning microscopy since we previously demonstrated that HCV NS5B-expressing PH5CH8 immortalized human hepatocyte cells were susceptible to DNA damage in the form of dsDNA breaks (23). ATM partially colocalized with NS5B in dispersed points throughout the cytoplasm (Fig. 5B), similar to the subcellular localization of HCV NS3-4A and ATM. Furthermore, Chk2 also partially colocalized with NS5B in the perinuclear region and in dispersed points in the nucleus (Fig. 5C). To determine whether endogenous ATM binds to NS5B, lysates from Oc or

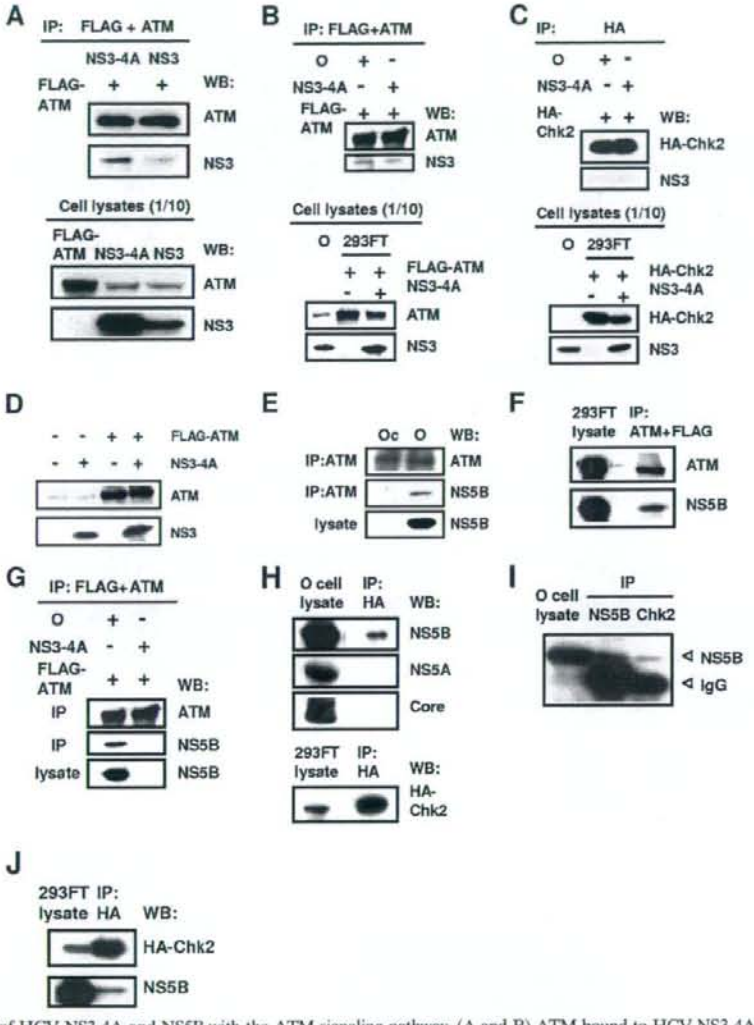

FIG. 6. Interaction of HCV NS3-4A and NS5B with the ATM signaling pathway. (A and B) ATM bound to HCV NS3-4A. (A) 293FT cells were transfected with 4 μg of pCX4bsr/NS3-4A (O), 4 μg of pCX4bsr/NS3 (O), or 4 μg of pcDNA3-FLAG-ATMwt. The cell lysates of expressed FLAG-ATM were mixed with lysates expressing either NS3-4A or NS3. The cell lysates were immunoprecipitated with both anti-FLAG (M2) and anti-ATM (2C1) antibodies, followed by immunoblotting analysis using either anti-ATM (2C1) or anti-HCV NS3 antibody. The results of Western blot analysis of 1/10 of the cellular lysates with anti-ATM or anti-NS3 antibody are also shown. (B) 293FT cells were cotransfected with 4 μg of pcDNA3-FLAG-ATMwt and/or 4 μg of pCX4bsr/NS3-4A (O). The cell lysates of expressed FLAG-ATM alone were mixed with the O cell lysates. Immunoprecipitation and Western blot analysis were performed as described in panel A. (C) Chk2 did not bind to NS3-4A. 293FT cells were cotransfected with 4 μg of pcDNA3-HA-Chk2wt and/or 4 μg of pCX4bsr/NS3-4A (O). The cell lysates of expressed HA-Chk2 alone were mixed with the O cell lysates. The cell lysates were immunoprecipitated with anti-HA antibody (3F10), followed by Western blot analysis using either anti-HA (HA-7) or anti-HCV NS3 antibody. The results of Western blot analysis of 1/10 of the cellular lysates with anti-HA or anti-NS3 antibody are also shown. (D) ATM was not cleaved by HCV NS3-4A protease. 293FT cells were cotransfected with 4 μg of pCX4bsr/NS3-4A (O) and/or 4 μg of pcDNA3-FLAG-ATMwt. The results of Western blot analysis of cellular lysates with anti-ATM or anti-NS3 antibody are shown. (E to G) ATM bound to HCV NS5B. (E) The lysates of O or Oc cells were immunoprecipitated with anti-ATM antibody (2C1), followed by immunoblotting analysis using either anti-ATM or anti-HCV NS5B antibody (no. 14). The results of Western blot analysis of 1/10 of the cellular lysates with anti-NS5B antibody are also shown. (F) 293FT cells were cotransfected with 4 μg of pCX4bsr/NS5B (1B-1) and 4 μg of pcDNA3-FLAG-ATMwt. The cell lysates were immunoprecipitated with both anti-FLAG and anti-ATM antibodies, followed by immunoblotting analysis using either anti-ATM or anti-HCV NS5B antibody. (G) Western Blot analysis was performed with anti-NS5B antibody, reusing the same blotted membrane that was used for panel B. (H to J) Chk2 bound to HCV NS5B. (H) 293FT cells were cotransfected with 4 μg of pcDNA3-HA-Chk2wt. The cell lysates of expressed HA-Chk2 were mixed with the O cell lysates and were immunoprecipitated with anti-HA antibody (3F10), followed by immunoblotting analysis using anti-HCV NS5B, anti-HCV NS5A (no. 8926), anti-HCV core protein (CP-9 and CP-11 mixture), or anti-HA (HA-7) antibody. The results of Western blot analysis of 1/10 of the cellular lysates with the same antibodies are also shown. (I) The lysates of O cells were immunoprecipitated with anti-NS5B or anti-Chk2 antibody (DCS-273), followed by immunoblotting analysis using anti-HCV NS5B antibody. The result of Western blot analysis of 1/10 of the cellular lysates with anti-NS5B antibody is also shown. (J) 293FT cells were cotransfected with 4 μg of pCX4bsr/NS5B (1B-1) and 4 μg of pcDNA3-HA-Chk2wt. The cell lysates were immunoprecipitated with anti-HA antibody (3F10), followed by immunoblotting analysis using either anti-HA (HA-7) or anti-HCV NS5B antibody. IP, immunoprecipitation; WB, Western blotting; IgG, immunoglobulin G.

O cells were immunoprecipitated with anti-ATM antibody, and then immunoblotting analysis using either anti-ATM or anti-NS5B antibody was performed. The results revealed that endogenous ATM bound to endogenous NS5B (Fig. 6E). Furthermore, we confirmed that ATM bound to NS5B in immunoprecipitation analysis using lysates from 293FT cells, in which NS5B (1B-1 strain) and FLAG-tagged ATM were overexpressed (Fig. 6F). Similarly, we confirmed that FLAG-tagged ATM bound to NS5B derived from O cell lysates in immunoprecipitation analysis using lysates from 293FT cells in which FLAG-tagged ATM was overexpressed (Fig. 6G). Finally, to determine which HCV protein binds to Chk2, the 293FT cell lysates of overexpressed HA-Chk2 were mixed with the O cell lysates and were immunoprecipitated with anti-HA antibody, followed by Western blot analysis using anti-HCV NS5B, anti-HCV NS5A, anti-HCV core protein, or anti-HA antibody. Consistent with the immunofluorescence result that Chk2 partially colocalized with NS5B (Fig. 5C), we observed that HA-tagged Chk2 bound to NS5B (Fig. 6H). Importantly, we found that endogenous Chk2 bound to endogenous NS5B derived from O cells (Fig. 6I). In addition, HA-tagged Chk2 bound to NS5B in immunoprecipitation analysis using lysates from 293FT cells in which NS5B (1B-1 strain) and HA-tagged Chk2 were overexpressed (Fig. 6J). Thus, Chk2 also interacted with NS5B as well as ATM. Taking these results together, we conclude that HCV targets ATM and Chk2 DNA damage sensors and that the ATM signaling pathway is required for HCV RNA replication.

DISCUSSION

ATM has been implicated as a target of most DNA viruses, harboring their genomes in the form of dsDNA which can activate or inhibit the ATM signaling pathway (17). In this study, we have demonstrated for the first time that the ATM signaling pathway is required for HCV RNA replication even though HCV does not have a dsDNA genome, unlike DNA viruses. In this regard, Machida et al. previously proposed that HCV infection and the expression of HCV NS3 and core protein induced dsDNA breaks (18, 19). Furthermore, NS3 has DNA helicase activity by which it unwinds dsDNA, suggesting that NS3 affects host dsDNA (22, 25). Thus, HCV infection might trigger the activation of ATM without a dsDNA genome. In fact, we observed weak but significant phosphorylation of Chk2 at threonine 68, the specific marker for ATM activation, in the HCV RNA-replicating cells (O and sO cells) but not in the HCV-negative Oc and sOc cells (Fig. 3A), suggesting that the ATM-dependent DNA damage response is constantly stimulated in persistent HCV RNA-replicating cells. Furthermore, we demonstrated that ATM preferentially bound to NS3-4A over NS3 alone (Fig. 5B) and that ATM partially colocalized with NS3-4A in the perinuclear region, where HCV is known to form a replication complex and replicate itself, and in dispersed points throughout the cytoplasm (Fig. 5A), indicating the interaction of ATM with NS3-4A. Interestingly, Lai et al. very recently reported that NS3-4A impaired DNA repair and enhanced sensitivity to ionizing radiation through interaction with ATM (15). However, we observed an equivalent level of Chk2 phosphorylation at threonine 68, a direct downstream target of ATM (20, 21), in both HCV RNA-replicating cells (O cells) and HCV-negative cells (Oc cells) after treatment with adriamycin (Fig. 3A), suggesting that Chk2 phosphorylation by ATM is not impaired by HCV RNA replication. In this regard, Gaspar and Shenk also showed that human cytomegalovirus could inhibit a DNA damage response by mislocalizing ATM and phosphorylated Chk2 at threonine 68 to a cytoplasmic virus assembly zone, indicating that human cytomegalovirus blocked at the level of Chk2 (9). On the other hand, dsDNA triggers IFN immune defenses through retinoic acid-induced gene I, the mitochondrial antiviral signaling protein, or the DNA-dependent activator of IFN-regulatory factor (7, 26); and NS3-4A protease, which is known to cleave the mitochondrial antiviral signaling protein, can block it (26), suggesting that interaction of NS3-4A with ATM is partially involved in such a common antiviral signaling pathway. On the other hand, we previously demonstrated that HCV NS5B-expressing PH5CH8 immortalized human hepatocyte cells were susceptible to DNA damage in the form of dsDNA breaks (23). In this regard, we have found that HCV NS5B could bind to both ATM and Chk2 (Fig. 5B and C and 6E to J). Together, these results indicate that HCV might hijack ATM and Chk2 and utilize ATM and Chk2 for HCV RNA replication, thereby resulting in impairment of DNA repair, enhancement of mutation frequency, and development of hepatocellular carcinoma.

Finally, consistent with our finding that ATM was required for HCV RNA replication, an ATM kinase inhibitor efficiently suppressed genome-length HCV RNA replication at an EC_{50} of approximately 2 μM at 72 h after the treatment (Fig. 4A). Similarly, Lau et al. reported that the same ATM kinase inhibitor could suppress HIV-1 replication at an EC_{50} of approximately 2.3 μM (16). Importantly, the EC_{50} for HIV-1 replication is similar to that for HCV replication. Thus, this or other ATM kinase inhibitors may represent a novel approach for the clinical treatment of patients with chronic hepatitis C as well as AIDS patients.

ACKNOWLEDGMENTS

We thank D. Trono, R. Agami, R. Iggo, M. Kastan, S. J. Elledge, M. Kohara, A. Takamizawa, and M. Hijikata for the VSV-G-pseudotyped HIV-1-based vector system (pCMVR8.91 and pMDG2) and for pSUPER, pRDI292, pcDNA3-FLAG-ATM, and pcDNA3-HA-Chk2, and for anti-NS3 antibody, anti-NS5B antibody, anti-NS5A antibody, and 293FT cells. We also thank A. Morishita and T. Nakamura for their technical assistance.

This work was supported by a Grant-in-Aid for Young Scientists (B) from the Ministry of Education, Culture, Sports, Science and Technology (MEXT); by a Grant-in-Aid for Research on Hepatitis from the Ministry of Health, Labor, and Welfare of Japan; by the Ichiro Kanehara Foundation; and by a Research Fellowship from the Japan Society for the Promotion of Science.

REFERENCES

1. **Ariumi, Y., P. Turelli, M. Masutani, and D. Trono.** 2005. DNA damage sensors ATM, ATR, DNA-PKcs, and PARP-1 are dispensable for human immunodeficiency virus type 1 integration. J. Virol. **79:**2973–2978.
2. **Ariumi, Y., and D. Trono.** 2006. Ataxia-telangiectasia-mutated (ATM) protein can enhance human immunodeficiency virus type 1 replication by stimulating Rev. function. J. Virol. **80:**2445–2452.
3. **Ariumi, Y., M. Kuroki, K. Abe, H. Dansako, M. Ikeda, T. Wakita, and N. Kato.** 2007. DDX3 DEAD-box RNA helicase is required for hepatitis C virus RNA replication. J. Virol. **81:**13922–13926.
4. **Bridge, A. J., S. Pebernard, A. Ducraux, A.-L. Nicoulaz, and R. Iggo.** 2003. Induction of an interferon response by RNAi vectors in mammalian cells. Nat. Genet. **34:**263–264.

5. **Brummelkamp, T. R., R. Bernard, and R. Agami.** 2002. A system for stable expression of short interfering RNAs in mammalian cells. Science **296:**550–553.
6. **Canman, C. E., D.-S. Lim, K. A. Cimprich, Y. Taya, K. Tamai, K. Sakaguchi, E. Apella, M. B. Kastan, and J. D. Siliciano.** 1998. Activation of the ATM kinase by ionizing radiation and phosphorylation of p53. Science **281:**1677–1679.
7. **Cheng, G., J. Zhong, J. Chung, and F. V. Chisari.** 2007. Double-stranded DNA and double-stranded RNA induces a common antiviral signaling pathway in human cells. Proc. Natl. Acad. Sci. USA **104:**9035–9040.
8. **Dansako, H., M. Ikeda, and N. Kato.** 2007. Limited suppression of the interferon-beta production by hepatitis C virus serine protease in cultured human hepatocytes. FEBS J. **274:**4161–4176.
9. **Gaspar, M., and T. Shenk.** 2006. Human cytomegalovirus inhibits a DNA damage response by mislocalizing checkpoint proteins. Proc. Natl. Acad. Sci. USA **103:**2821–2826.
10. **Harper, J. W., and S. J. Elledge.** 2007. The DNA damage response: ten years after. Mol. Cell **28:**739–745.
11. **Ikeda, M., K. Abe, H. Dansako, T. Nakamura, K. Naka, and N. Kato.** 2005. Efficient replication of a full-length hepatitis C virus genome, strain O, in cell culture, and development of a luciferase reporter system. Biochem. Biophys. Res. Commun. **329:**1350–1359.
12. **Kato, N., M. Hijikata, Y. Ootsuyama, M. Nakagawa, S. Ohkoshi, T. Sugimura, and K. Shimotohno.** 1990. Molecular cloning of the human hepatitis C virus genome from Japanese patients with non-A, non-B hepatitis. Proc. Natl. Acad. Sci. USA **87:**9524–9528.
13. **Kato, N.** 2001. Molecular virology of hepatitis C virus. Acta Med. Okayama **55:**133–159.
14. **Kato, N., K. Sugiyama, K. Namba, H. Dansako, T. Nakamura, M. Takami, K. Naka, A. Nozaki, and K. Shimotohno.** 2003. Establishment of a hepatitis C virus subgenomic replicon derived from human hepatocytes infected in vitro. Biochem. Biophys. Res. Commun. **306:**756–766.
15. **Lai, C. K., K. S. Jeng, K. Machida, Y. S. Cheng, and M. M. Lai.** 2008. Hepatitis C virus NS3/4A protein interacts with ATM, impairs DNA repair and enhances sensitivity to ionizing radiation. Virology **370:**295–309.
16. **Lau, A., K. M. Swinbank, P. S. Ahmed, D. L. Taylor, S. P. Jackson, G. C. Smith, and M. J. O'Connor.** 2005. Suppression of HIV-1 infection by a small molecule inhibitor of the ATM kinase. Nat. Cell Biol. **7:**493–500.
17. **Lilley, C. E., R. A. Schwartz, and M. D. Weitzman.** 2007. Using or abusing: viruses and the cellular DNA damage response. Trends Microbiol. **15:**119–126.
18. **Machida, K., K. T. Cheng, V. M. Sung, S. Shimodaira, K. L. Lindsay, A. M. Levine, M. Y. Lai, and M. M. Lai.** 2004. Hepatitis C virus induces a mutator phenotype: enhanced mutations of immunoglobulin and protooncogenes. Proc. Natl. Acad. Sci. USA **101:**4262–4267.
19. **Machida, K., K. T. Cheng, V. M. Sung, K. J. Lee, A. M. Levine, and M. M. Lai.** 2004. Hepatitis C virus infection activates the immunologic (type II) isoform of nitric oxide synthase and thereby enhances DNA damage and mutations of cellular genes. J. Virol. **78:**8835–8843.
20. **Matsuoka, S., M. Huang, and S. J. Elledge.** 1998. Linkage of ATM to cell cycle regulation by the Chk2 protein kinase. Science **282:**1893–1897.
21. **Matsuoka, S., G. Rotman, A. Ogawa, Y. Shiloh, K. Tamai, and S. J. Elledge.** 2000. Ataxia telangiectasia-mutated phosphorylates Chk2 in vivo and in vitro. Proc. Natl. Acad. Sci. USA **97:**10389–10394.
22. **Myong, S., M. M. Bruno, A. M. Pyle, and T. Ha.** 2007. Spring-loaded mechanism of DNA unwinding by hepatitis C virus NS3 helicase. Science **317:**513–516.
23. **Naka, K., H. Dansako, N. Kobayashi, M. Ikeda, and N. Kato.** 2006. Hepatitis C virus NS5B delays cell cycle progression by inducing interferon-β via Toll-like receptor 3 signaling pathway without replicating viral genomes. Virology **346:**348–362.
24. **Naldini, L., U. Blömer, P. Gallay, D. Ory, R. Mulligan, F. H. Gage, I. M. Verma, and D. Trono.** 1996. In vivo gene delivery and stable transduction of nondividing cells by a lentiviral vector. Science **272:**263–267.
25. **Pang, P. S., E. Jankowsky, P. J. Planet, and A. M. Pyle.** 2002. The hepatitis C viral NS3 protein is a processive DNA helicase with cofactor enhanced RNA unwinding. EMBO J. **21:**1168–1176.
26. **Takaoka, A., Z. Wang, M. K. Choi, H. Yanai, H. Negishi, T. Ban, Y. Lu, M. Miyagishi, T. Kodama, K. Honda, Y. Ohba, and T. Taniguchi.** 2007. DAI (DLM-1/ZBP1) is a cytosolic DNA sensor and an activator of innate immune response. Nature **448:**501–505.
27. **Tanaka, T., N. Kato, M. J. Cho, and K. Shimotohno.** 1995. A novel sequence found at the 3′ terminus of hepatitis C virus genome. Biochem. Biophys. Res. Commun. **215:**744–749.
28. **Thomas, D. L.** 2000. Hepatitis C epidemiology. Curr. Top. Microbiol. Immunol. **242:**25–41.
29. **Wakita, T., T. Pietschmann, T. Kato, T. Date, M. Miyamoto, Z. Zhao, K. Murthy, A. Habermann, H. G. Kräusslich, M. Mizokami, R. Bartenschlager, and T. J. Liang.** 2005. Production of infectious hepatitis C virus in tissue culture from a cloned viral genome. Nat. Med. **11:**791–796.
30. **Zufferey, R., D. Nagy, R. J. Mandel, L. Naldini, and D. Trono.** 1997. Multiply attenuated lentiviral vector achieves efficient gene delivery in vivo. Nat. Biotechnol. **15:**871–875.

Short Communication

Virological characterization of the hepatitis C virus JFH-1 strain in lymphocytic cell lines

Kyoko Murakami,[1] Toshiro Kimura,[1] Motonao Osaki,[1] Koji Ishii,[1] Tatsuo Miyamura,[1] Tetsuro Suzuki,[1] Takaji Wakita[1] and Ikuo Shoji[1,2]

Correspondence
Ikuo Shoji
ishoji@med.kobe-u.ac.jp

[1]Department of Virology II, National Institute of Infectious Diseases, 1-23-1 Toyama, Shinjuku-ku, Tokyo 162-8640, Japan

[2]Division of Microbiology, Kobe University Graduate School of Medicine, 7-5-1 Kusunoki-cho, Chuo-ku, Kobe, Hyogo 650-0017, Japan

Received 25 November 2007
Accepted 18 March 2008

While hepatocytes are the major site of hepatitis C virus (HCV) infection, a number of studies have suggested that HCV can replicate in lymphocytes. However, *in vitro* culture systems to investigate replication of HCV in lymphocytic cells are severely limited. Robust HCV culture systems have been established using the HCV JFH-1 strain and Huh-7 cells. To gain more insights into the tissue tropism of HCV, we investigated the infection, replication, internal ribosome entry site (IRES)-dependent translation and polyprotein processing of the HCV JFH-1 strain in nine lymphocytic cell lines. HCV JFH-1 failed to infect lymphocytes and replicate, but exhibited efficient polyprotein processing and IRES-dependent translation in lymphocytes as well as in Huh-7 cells. Our results suggest that lymphocytic cells can support HCV JFH-1 translation and polyprotein processing, but may lack some host factors essential for HCV JFH-1 infection and replication.

Hepatitis C virus (HCV) is a major cause of chronic hepatitis, liver cirrhosis and hepatocellular carcinoma (Choo *et al.*, 1989; Saito *et al.*, 1990). Infection with HCV is frequently associated with B-cell-related diseases, such as mixed cryoglobulinaemia and non-Hodgkin's lymphoma (Hausfater *et al.*, 2000). A number of studies have suggested that HCV can replicate not only in hepatocytes, but also in lymphocytes (Ducoulombier *et al.*, 2004; Karavattathayyil *et al.*, 2000, Lerat *et al.*, 1998), whereas the determinants of HCV tropism are still unknown. The development of HCV strain JFH-1, which generates infectious HCV in culture, has made an important contribution to the study of the HCV life cycle (Lindenbach *et al.*, 2005; Wakita *et al.*, 2005; Zhong *et al.*, 2005). The HCV life cycle is divided into several steps. After entry into the cell and uncoating, the HCV life cycle leads to translation, polyprotein processing, RNA replication, virion assembly, transport and release. The JFH-1 subgenomic replicon can replicate in non-hepatic cell lines, such as HeLa cells and 293 cells, suggesting that the host factors required for HCV replication are not hepatocyte-specific (Kato *et al.*, 2005b). The SB strain of HCV (genotype 2b strain) was isolated from an HCV-infected non-Hodgkin's B-cell lymphoma and has been reported to infect B and T cells (Kondo *et al.*, 2007; Sung *et al.*, 2003). The virus titres of the SB strain in lymphocytes were, however, lower than those of JFH-1 in Huh-7 cells and the expression of HCV proteins was not confirmed (Kondo *et al.*, 2007). It is unknown whether HCV JFH-1 can infect and replicate in lymphocytes. To gain more insight into the tissue tropism of HCV infection, we investigated the infection, replication, IRES-dependent translation and polyprotein processing of the JFH-1 strain in nine lymphocytic cell lines.

We first sought to determine whether HCV JFH-1 can infect lymphocytic cell lines. We chose nine lymphocytic cell lines derived from Burkitt's lymphoma, the EBV-immortalized human B cell line, lymphoblasts and acute T-cell leukaemia. C1R, IB4, Namalwa, P3HR1 and Raji cells were Epstein–Barr virus (EBV)-positive (Table 1). Infectious HCV was generated from HCV JFH-1 RNA in Huh-7 cells (Shirakura *et al.*, 2007; Wakita *et al.*, 2005) and the calculation of the 50 % tissue culture infectious dose ($TCID_{50}$) was based on methods described previously (Lindenbach *et al.*, 2005). These cell lines (1×10^5 cells per well of a six-well plate) were incubated with 2 ml inoculum (5×10^3 or 5×10^4 $TCID_{50}$ ml^{-1}) for 3 h, washed three times with PBS, and cultured in fresh medium. The culture medium was changed every 2 days. Cells were harvested at 0 (3 h post-infection [p.i.]), 4 and 8 day p.i. HCV core antigen within cells was quantified by immunoassay (Ortho HCV-core ELISA kit; Ortho-Clinical Diagnostics). As shown in Fig. 1(a), increasing the HCV titre of the inoculum resulted in a 7.2-fold increase in the levels of HCV core protein in Huh-7 cells at 3 h p.i. Increasing the HCV titre of the inoculum resulted in a 1.5- to 3.2-fold increase in the levels of the core protein in C1R, BL41,

Table 1. Summary of the virological characterization of HCV JFH-1 in lymphocytes

Name	Source	EBV	Transfection			Concentration of G418 for selection (μg ml^{-1})	HCVcc infection	HCV-RNA replication	Translation*		Polyprotein processing†
			Buffer	Program	Efficiency				HCV-IRES	EMCV-IRES	
Bjab	Burkitt's lymphoma	−	T	T−16	>90 %	600–800	−	−	+	++	+
BL41	Burkitt's lymphoma	−	V	I−10	60–70 %	1000	−	−	+	++	ND
C1R	B lymphoblast	+	V	T−20	70–80 %	100	−	−	++++	++++	+
IB4	Lymphoblastoid	+	V	T−20	80–90 %	1000	−	−	+++	++++	+
Jurkat	Acute T cell leukaemia	−	V	I−10	60–70 %	600	−	−	++	+	ND
Namalwa	Burkitt's lymphoma	+	V	M−13	60–70 %	600–800	−	−	+++	++++	+
P3HR1	Burkitt's lymphoma	+	V	A−23	60–70 %	800	−	−	+++	++++	ND
Raji	Burkitt's lymphoma	+	V	T−27	70–80 %	800	−	−	++	++++	+
Ramos	Burkitt's lymphoma	−	V	M−13	40–60 %	400	−	−	+	+	ND
Huh7	Hepatoma	−	T	T−14	70–80 %	500	+	+	+++	+++	+

*+, <0.25 fold IRES activity of Huh-7; ++, 0.25–0.75 fold; +++, 0.75–1.5-fold; ++++, >1.5-fold.
†ND, Not determined.

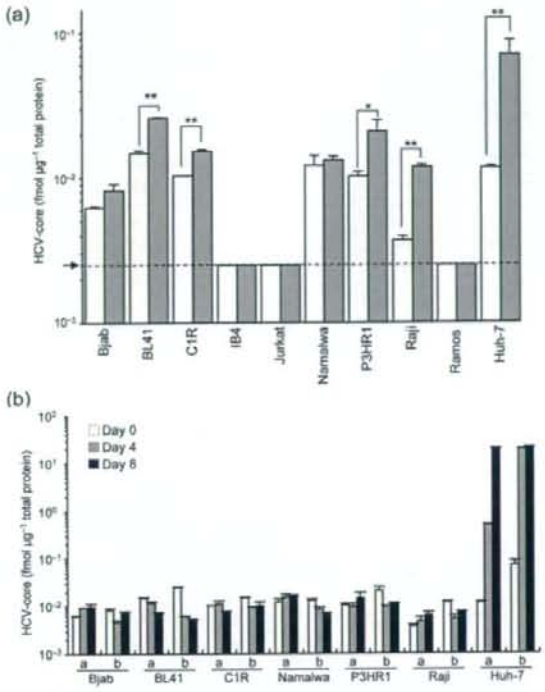

Fig. 1. HCV infection assay. (a) HCV core protein levels 3 h after infection. A total of 1×10^5 cells were infected with 2 ml of the inoculum (5×10^3 [white bars] or 5×10^4 [grey bars] $TCID_{50}$ ml^{-1}) for 3 h at 37 °C and harvested at 3 h p.i. HCV core protein in cell lysate was quantified by ELISA. The average values with standard deviations from triplicate samples are shown. The cut-off value of the immunoassay is indicated by an arrow and a dotted line. The difference between low m.o.i. (white bars) and high m.o.i. (grey bars) was significant (*, $P<0.05$; **, $P<0.01$, Student's *t*-test). (b) Time-course of HCV core protein levels after infection. In total, 1×10^5 cells were infected with 2 ml of the inoculum (5×10^3 [a] or 5×10^4 [b] $TCID_{50}$ ml^{-1}) for 3 h and harvested at 0, 4 and 8 days p.i. HCV core protein in cell lysate was quantified by ELISA. Average values ± SD from triplicate samples are shown.

P3HR1 and Raji cells, suggesting that HCV can bind to these cell lines (Fig. 1a). In contrast, the levels of HCV core protein in IB4, Jurkat and Ramos cells at 3 h p.i. were below the detection limits and there were no significant differences in the levels of the core protein in Bjab cells and Namalwa cells, suggesting that HCV binding to these cells was very inefficient (Fig. 1a). Moreover, the levels of HCV core protein increased in Huh-7 cells but, in the case of all lymphocytic cell lines, including Raji cells, the core titre did not increase at day 4 and 8 p.i., suggesting that HCV JFH-1 does not infect and/or replicate efficiently in these lymphocytic cell lines (Fig. 1b).

To assess the replication of JFH-1 in our lymphocytic cell lines, we utilized the HCV replicon system. To visualize the

replicating cells, a reporter replicon plasmid was constructed as follows. The gene encoding green fluorescence protein (GFP) was fused to the neomycin resistance gene using an overlap PCR amplification technique and the fusion product was inserted into pSGR-JFH1. The resultant plasmid was pSGR-GFPneo-JFH1. This plasmid was linearized with *Xba*I and used as a template for *in vitro* transcription using an AmpliScribe T7 High Yield Transcription kit (Epicentre Biotechnologies). RNA was transfected with high transfection efficiency and low cytotoxicity using the Nucleofector system (Amaxa Biosystems) (Coughlin *et al.*, 2004; Miyahara *et al.*, 2005; Van De Parre *et al.*, 2005). The transfection efficiencies ranged from 60 to 80 % after optimization of transfection conditions (Table 1). GFP expression was monitored periodically during the selection of HCV-replicon cells by G418 (Table 1). The GFP-expressing cells were detected at day 3 post-transfection (p.t.) in Huh-7, P3HR1, Raji, C1R and Namalwa cells. The rate of GFP expression in Huh-7 cells was more than 50 %. The rate of GFP-expression in lymphocytic cell lines was less than 1 %, despite the high transfection efficiencies. After 3 weeks of G418 selection, SGR-GFPneo-JFH1 replicon cells were established in Huh-7 cells, but not in lymphocytic cells. These data suggest that JFH-1 subgenomic replicon RNA cannot replicate in the lymphocytic cell lines.

To facilitate quantification of replication, we performed luciferase assays using subgenomic replicon RNA (SGR-JFH1/Luc) carrying firefly luciferase as a reporter. SGR-JFH1/Luc RNA was *in vitro*-transcribed using the linearized pSGR-JFH1/Luc (Kato *et al.*, 2005a) as template DNA. Cells were harvested at 4, 24, 48 and 72 h p.t. and luciferase activities were assayed with luciferase assay reagent (Promega). Assays were performed at least in triplicate. There were significant differences in luciferase activities at 4 h p.t. among the cell lines, probably because there were differences in transfection efficiencies and the doubling time of the cell lines. Thus, the replication activity was expressed relative to the reporter activity determined 4 h p.t. for each cell line, which was set to 1 (Fig. 2a). HCV subgenomic replicon RNA efficiently replicated in Huh-7 cells (Fig. 2a). Replication-deficient subgenomic replicon RNA encoding a GDD to GND mutation in NS5B served as a negative control in Huh-7 cells. The luciferase activities of replication-deficient subgenomic replicon RNA in lymphocytic cell lines also decreased rapidly (data not shown). As shown in Fig. 2(a), the luciferase activities of HCV subgenomic replicon RNA in lymphocytic cell lines decreased rapidly, suggesting that HCV subgenomic replicon RNA did not replicate efficiently in lymphocytic cell lines. Thus, these two different replicon assays demonstrated that the HCV JFH-1 subgenomic replicon failed to replicate in our lymphocytic cell lines.

To determine which steps of the HCV life cycle are impaired, we further examined translation and polyprotein processing. At first, we assessed HCV IRES-dependent translational efficiencies in the lymphocytic cell lines. Cells were co-transfected with the subgenomic replicon RNA (SGR-JFH1/Luc) and a capped RNA encoding *Renilla* luciferase (cap-luc). Cap-luc RNA was *in vitro*-transcribed using a T7 mMessage mMachine kit (Ambion). The HCV IRES activities in IB4, Namalwa and P3HR1 cells were as high as in Huh-7 cells. The HCV IRES activities in Jurkat and Raji cells were about 50 % of those in Huh-7 cells, and the HCV IRES activities in Bjab, BL41 and Ramos cells were less than 25 % of those in Huh-7 cells. On the other hand, the HCV IRES activity in C1R cells was about twofold higher than in Huh-7 cells (Fig. 2b). Replication-deficient subgenomic replicon RNA encoding a GDD to GND mutation in NS5B showed a luciferase activity level similar to that of the wild-type, suggesting that the luciferase activity at 4 h after transfection reflected translational levels but not replication levels (data not shown). Our data indicate high HCV IRES activities in all cell lines, except in Bjab, BL41 and Ramos.

The HCV polyprotein is translated in subgenomic replicon cells in an encephalomyocarditis virus (EMCV) IRES-dependent manner. To rule out the possibility that the EMCV IRES-dependent translation is impaired in lymphocytic cell lines, we assessed the EMCV IRES-dependent translational efficiencies. We assayed EMCV IRES activity using EMCV IRES-driven luciferase RNA (EMC-luc) and Cap-luc RNA. The EMCV IRES activity was five- to tenfold higher in C1R, Namalwa, IB4 and P3HR1 than in Huh-7 cells (Fig. 2c). From these results, HCV IRES and EMCV IRES exhibited sufficient translational activity in C1R, Namalwa, P3HR1 and Raji cells, suggesting that IRES-dependent translation was not impaired in these lymphocytic cell lines.

To determine whether HCV polyprotein is properly processed in lymphocytes, we examined the processing of HCV non-structural (NS) proteins. The construct pSGR-JFH1/Luc expresses the polyprotein NS3-NS4A-NS4B-NS5A-NS5B. The HCV NS3/4A protease is responsible for proteolytic processing at each cleavage site. We used the eukaryotic transient-expression system based on a recombinant vaccinia virus carrying bacteriophage T7 RNA polymerase (T7vac) (Fuerst *et al.*, 1989). To express the SGR-JFH1/Luc encoding HCV NS proteins, 5×10^6 cells were transfected with 5 μg pSGR-JFH1/Luc and infected with 2.5×10^9 p.f.u. T7vac, harvested at 24 h p.i., and analysed by Western blotting. Completely processed NS3, NS5A and NS5B proteins were detected in Bjab, Raji, IB4 and Namalwa cells as well as in pSGR-JFH1/Luc-transfected Huh-7 cells and HCV-JFH1-infected Huh-7 cells (Fig. 2c). The unprocessed polyprotein was not detected by immunoblotting in these lymphocytic cell lines (data not shown). These results suggest that the HCV polyprotein is efficiently processed in these lymphocytic cells.

In this study, we demonstrated that HCV JFH-1 failed to infect and replicate in nine lymphocytic cell lines. In contrast, HCV IRES-dependent translation and polyprotein processing by NS3/NS4A protease functioned properly

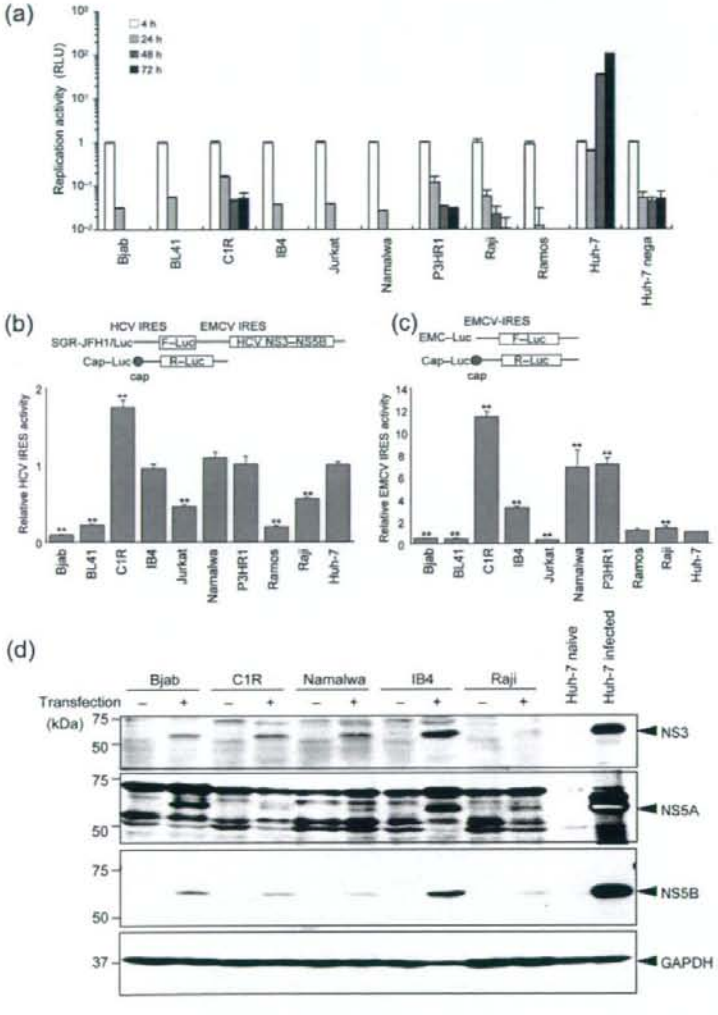

Fig. 2. Replication, HCV IRES-dependent translational efficiencies and polyprotein processing. (a) Subgenomic replicon assay. JFH-1 subgenomic replicon RNA was transfected into several cell lines and harvested at 4, 24, 48 and 72 h p.t. The replication activity was expressed relative to the reporter activity determined 4 h p.t. for each cell line, which was set to 1. RLU, Relative luciferase units; Huh-7 nega, Huh-7 cells transfected with SGR-JFH1/Luc GND, served as a negative control. (b) HCV IRES-dependent translational efficiency. To determine the HCV IRES activities, we co-transfected cells with SGR-JFH1/Luc RNA and Cap-Renilla luciferase RNA. The IRES activity of each cell line is expressed in relation to Huh-7 IRES activity, that is, as the ratio of HCV IRES-driven firefly luciferase activity to cap-driven *Renilla* luciferase activity. The difference in HCV IRES activity between Huh-7 cells and the lymphocytic cell line was significant (**, $P<0.01$, Student's *t*-test). (c) EMCV IRES-dependent translational efficiency. To determine the EMCV IRES activities, we co-transfected cells with EMCV–firefly luciferase RNA and Cap-Renilla luciferase RNA. The IRES activity of each cell line is expressed in relation to Huh-7 IRES activity, that is, as the ratio of EMCV IRES-driven firefly luciferase activity to cap-driven *Renilla* luciferase activity. The difference in EMCV IRES activity between Huh-7 cell and the lymphocytic cell line was significant (**, $P<0.01$, Student's *t*-test). (d) Polyprotein processing by NS3/4A protease in lymphocytic cell lines. pSGR-JFH1/Luc-transfected cells were infected with T7vac and harvested at 24 h p.i. HCV NS proteins, NS3, NS5A and NS5B were detected by using anti-NS3 rabbit polyclonal antibody (PAb), anti-NS5A rabbit PAb and anti-NS5B rabbit PAb. Arrowheads indicate the processed NS3, NS5A and NS5B proteins, respectively.

in these cells. Moreover, subgenomic replicon RNA failed to replicate in these cell lines. Our data suggest that lymphocytic cell lines may lack some host factors required for infection and replication of HCV-JFH1.

Viral entry often requires sequential interactions between viral proteins and several cellular factors. Several molecules (CD81, Claudin-1, Scavenger receptor class B member IR, LDL-receptor and glycosaminoglycans) have been reported to be involved in HCV binding and entry (Barth *et al.*, 2003; Evans *et al.*, 2007; Pileri *et al.*, 1998; Scarselli *et al.*, 2002). Further investigation will be required to clarify HCV binding and entry into lymphocytic cell lines.

HCV IRES and EMCV IRES exhibited sufficient translational activities in C1R, IB4, P3HR1, Namalwa and Raji cells. All these cell lines are EBV-positive. EBV-encoded nuclear antigen (EBNA1) has been reported to support HCV replication (Sugawara *et al.*, 1999). Two small EBV-encoded RNA species (EBERs) bind to the HCV IRES region (Wood *et al.*, 2001). These findings raise the possibility that HCV IRES activities may be modified by the EBV genome.

HCV JFH-1 subgenomic replicon RNA could not replicate in all lymphocytes tested in this study. The HCV SB strain, however, has been reported to infect Raji, Daudi, Molt-4

and Jurkat cells (Kondo *et al.*, 2007; Sung *et al.*, 2003). Still unknown is how hepatotropism and lymphotropism of HCV are determined. The GB virus B (GBV-B) is most closely related to HCV and the GBV-B infection of tamarins has been proposed as a good surrogate model for chronic hepatitis C (Bukh *et al.*, 2001; Jacob *et al.*, 2004; Lanford *et al.*, 2003; Martin *et al.*, 2003). A recent report has shown that GBV can disseminate to not only liver but also a variety of extrahepatic tissues such as haematolymphoid and genital tissues in tamarins (Ishii *et al.*, 2007). Viral RNA cloned from plasma and liver from the tamarins showed no sequence heterogeneity, suggesting that host factors determine the pleiotropism (Ishii *et al.*, 2007). It remains unclear how host factors and/or viral factors determine the tissue tropism of HCV. Further studies will be required to clarify the molecular mechanisms of HCV tissue tropism.

Acknowledgements

The authors gratefully acknowledge Drs Sanae Machida (Saitama Medical School, Saitama, Japan), Shizuko Harada (NIID, Tokyo, Japan) and Isao Hamaguchi (NIID, Tokyo, Japan) for the cell lines, and Dr Hideki Aizaki (NIID, Tokyo, Japan) for helpful discussion. This work was supported in part by grants-in-aid from the Ministry of Health, Labour and Welfare, by a grant for Research on Health Sciences focusing on Drug Innovation from the Japan Health Sciences Foundation, and by grant-in aid for young scientists (B).

References

Barth, H., Schafer, C., Adah, M. I., Zhang, F., Linhardt, R. J., Toyoda, H., Kinoshita-Toyoda, A., Toida, T., Van Kuppevelt, T. H. & other authors (2003). Cellular binding of hepatitis C virus envelope glycoprotein E2 requires cell surface heparan sulfate. *J Biol Chem* **278**, 41003–41012.

Bukh, J., Apgar, C. L., Govindarajan, S. & Purcell, R. H. (2001). Host range studies of GB virus-B hepatitis agent, the closest relative of hepatitis C virus, in New World monkeys and chimpanzees. *J Med Virol* **65**, 694–697.

Choo, Q. L., Kuo, G., Weiner, A. J., Overby, L. R., Bradley, D. W. & Houghton, M. (1989). Isolation of a cDNA clone derived from a blood-borne non-A, non-B viral hepatitis genome. *Science* **244**, 359–362.

Coughlin, C. M., Vance, B. A., Grupp, S. A. & Vonderheide, R. H. (2004). RNA-transfected CD40-activated B cells induce functional T-cell responses against viral and tumor antigen targets: implications for pediatric immunotherapy. *Blood* **103**, 2046–2054.

Ducoulombier, D., Roque-Afonso, A. M., Di Liberto, G., Penin, F., Kara, R., Richard, Y., Dussaix, E. & Feray, C. (2004). Frequent compartmentalization of hepatitis C virus variants in circulating B cells and monocytes. *Hepatology* **39**, 817–825.

Evans, M. J., von Hahn, T., Tscherne, D. M., Syder, A. J., Panis, M., Wolk, B., Hatziioannou, T., McKeating, J. A., Bieniasz, P. D. & Rice, C. M. (2007). Claudin-1 is a hepatitis C virus co-receptor required for a late step in entry. *Nature* **446**, 801–805.

Fuerst, T. R., Fernandez, M. P. & Moss, B. (1989). Transfer of the inducible *lac* repressor/operator system from *Escherichia coli* to a vaccinia virus expression vector. *Proc Natl Acad Sci U S A* **86**, 2549–2553.

Hausfater, P., Rosenthal, E. & Cacoub, P. (2000). Lymphoproliferative diseases and hepatitis C virus infection. *Ann Med Interne (Paris)* **151**, 53–57.

Ishii, K., Iijima, S., Kimura, N., Lee, Y. J., Ageyama, N., Yagi, S., Yamaguchi, K., Maki, N., Mori, K. & other authors (2007). GBV-B as a pleiotropic virus: distribution of GBV-B in extrahepatic tissues *in vivo*. *Microbes Infect* **9**, 515–521.

Jacob, J. R., Lin, K. C., Tennant, B. C. & Mansfield, K. G. (2004). GB virus B infection of the common marmoset (*Callithrix jacchus*) and associated liver pathology. *J Gen Virol* **85**, 2525–2533.

Karavattathayyil, S. J., Kalkeri, G., Liu, H. J., Gaglio, P., Garry, R. F., Krause, J. R. & Dash, S. (2000). Detection of hepatitis C virus RNA sequences in B-cell non-Hodgkin lymphoma. *Am J Clin Pathol* **113**, 391–398.

Kato, T., Date, T., Miyamoto, M., Sugiyama, M., Tanaka, Y., Orito, E., Ohno, T., Sugihara, K., Hasegawa, I. & other authors (2005a). Detection of anti-hepatitis C virus effects of interferon and ribavirin by a sensitive replicon system. *J Clin Microbiol* **43**, 5679–5684.

Kato, T., Date, T., Miyamoto, M., Zhao, Z., Mizokami, M. & Wakita, T. (2005b). Nonhepatic cell lines HeLa and 293 support efficient replication of the hepatitis C virus genotype 2a subgenomic replicon. *J Virol* **79**, 592–596.

Kondo, Y., Sung, V. M., Machida, K., Liu, M. & Lai, M. M. (2007). Hepatitis C virus infects T cells and affects interferon-gamma signaling in T cell lines. *Virology* **361**, 161–173.

Lanford, R. E., Chavez, D., Notvall, L. & Brasky, K. M. (2003). Comparison of tamarins and marmosets as hosts for GBV-B infections and the effect of immunosuppression on duration of viremia. *Virology* **311**, 72–80.

Lerat, H., Rumin, S., Habersetzer, F., Berby, F., Trabaud, M. A., Trepo, C. & Inchauspe, G. (1998). In vivo tropism of hepatitis C virus genomic sequences in hematopoietic cells: influence of viral load, viral genotype, and cell phenotype. *Blood* **91**, 3841–3849.

Lindenbach, B. D., Evans, M. J., Syder, A. J., Wolk, B., Tellinghuisen, T. L., Liu, C. C., Maruyama, T., Hynes, R. O., Burton, D. R. & other authors (2005). Complete replication of hepatitis C virus in cell culture. *Science* **309**, 623–626.

Martin, A., Bodola, F., Sangar, D. V., Goettge, K., Popov, V., Rijnbrand, R., Lanford, R. E. & Lemon, S. M. (2003). Chronic hepatitis associated with GB virus B persistence in a tamarin after intrahepatic inoculation of synthetic viral RNA. *Proc Natl Acad Sci U S A* **100**, 9962–9967.

Miyahara, Y., Naota, H., Wang, L., Hiasa, A., Goto, M., Watanabe, M., Kitano, S., Okumura, S., Takemitsu, T. & other authors (2005). Determination of cellularly processed HLA-A2402-restricted novel CTL epitopes derived from two cancer germ line genes, MAGE-A4 and SAGE. *Clin Cancer Res* **11**, 5581–5589.

Pileri, P., Uematsu, Y., Campagnoli, S., Galli, G., Falugi, F., Petracca, R., Weiner, A. J., Houghton, M., Rosa, D. & other authors (1998). Binding of hepatitis C virus to CD81. *Science* **282**, 938–941.

Saito, I., Miyamura, T., Ohbayashi, A., Harada, H., Katayama, T., Kikuchi, S., Watanabe, Y., Koi, S., Onji, M. & other authors (1990). Hepatitis C virus infection is associated with the development of hepatocellular carcinoma. *Proc Natl Acad Sci U S A* **87**, 6547–6549.

Scarselli, E., Ansuini, H., Cerino, R., Roccasecca, R. M., Acali, S., Filocamo, G., Traboni, C., Nicosia, A., Cortese, R. & Vitelli, A. (2002). The human scavenger receptor class B type I is a novel candidate receptor for the hepatitis C virus. *EMBO J* **21**, 5017–5025.

Shirakura, M., Murakami, K., Ichimura, T., Suzuki, R., Shimoji, T., Fukuda, K., Abe, K., Sato, S., Fukasawa, M. & other authors (2007).

E6AP ubiquitin ligase mediates ubiquitylation and degradation of hepatitis C virus core protein. *J Virol* **81**, 1174–1185.

Sugawara, Y., Makuuchi, M., Kato, N., Shimotohno, K. & Takada, K. (1999). Enhancement of hepatitis C virus replication by Epstein–Barr virus-encoded nuclear antigen 1. *EMBO J* **18**, 5755–5760.

Sung, V. M., Shimodaira, S., Doughty, A. L., Picchio, G. R., Can, H., Yen, T. S., Lindsay, K. L., Levine, A. M. & Lai, M. M. (2003). Establishment of B-cell lymphoma cell lines persistently infected with hepatitis C virus in vivo and in vitro: the apoptotic effects of virus infection. *J Virol* **77**, 2134–2146.

Van De Parre, T. J., Martinet, W., Schrijvers, D. M., Herman, A. G. & De Meyer, G. R. (2005). mRNA but not plasmid DNA is efficiently transfected in murine J774A.1 macrophages. *Biochem Biophys Res Commun* **327**, 356–360.

Wakita, T., Pietschmann, T., Kato, T., Date, T., Miyamoto, M., Zhao, Z., Murthy, K., Habermann, A., Krausslich, H. G. & other authors (2005). Production of infectious hepatitis C virus in tissue culture from a cloned viral genome. *Nat Med* **11**, 791–796.

Wood, J., Frederickson, R. M., Fields, S. & Patel, A. H. (2001). Hepatitis C virus 3′X region interacts with human ribosomal proteins. *J Virol* **75**, 1348–1358.

Zhong, J., Gastaminza, P., Cheng, G., Kapadia, S., Kato, T., Burton, D. R., Wieland, S. F., Uprichard, S. L., Wakita, T. & Chisari, F. V. (2005). Robust hepatitis C virus infection *in vitro*. *Proc Natl Acad Sci U S A* **102**, 9294–9299.

Hepatitis C Virus–Infected Hepatocytes Extrinsically Modulate Dendritic Cell Maturation To Activate T Cells and Natural Killer Cells

Takashi Ebihara,[1] Masashi Shingai,[1] Misako Matsumoto,[1] Takaji Wakita,[2] and Tsukasa Seya[1]

Dendritic cell maturation critically modulates antiviral immune responses, and facilitates viral clearance. Hepatitis C virus (HCV) is characterized by its high predisposition to persistent infection. Here, we examined the immune response of human monocyte-derived dendritic cells (MoDCs) to the JFH1 strain of HCV, which can efficiently replicate in cell culture. However, neither HCV RNA replication nor antigen production was detected in MoDCs inoculated with JFH1. None of the indicators of HCV interacting with MoDCs we evaluated were affected, including expression of maturation markers (CD80, 83, 86), cytokines (interleukin-6 and interferon-beta), the mixed lymphocyte reaction, and natural killer (NK) cell cytotoxicity. Strikingly, MoDCs matured by phagocytosing extrinsically-infected vesicles containing HCV-derived double-stranded RNA (dsRNA). When MoDCs were cocultured with HCV-infected apoptotic Huh7.5.1 hepatic cells, there was increased CD86 expression and interleukin-6 and interferon-beta production in MoDCs, which were characterized by the potential to activate NK cells and induce $CD4^+$ T cells into the T helper 1 type. Lipid raft-dependent phagocytosis of HCV-infected apoptotic vesicles containing dsRNA was indispensable to MoDC maturation. Colocalization of dsRNA with Toll-like receptor 3 (TLR3) in phagosomes suggested the importance of TLR3 signaling in the MoDC response against HCV. ***Conclusion:*** **The JFH1 strain does not directly stimulate MoDCs to activate T cells and NK cells, but phagocytosing HCV-infected apoptotic cells and their interaction with the TLR3 pathway in MoDCs plays a critical role in MoDC maturation and reciprocal activation of T and NK cells.** (HEPATOLOGY 2008;48:48-58.)

Abbreviations: CPZ, chlorpromazine; CTL, cytotoxic T lymphocyte; DC, dendritic cell; DC-SIGN, dendritic cell-specific intercellular adhesion molecule 3-grabbing nonintegrin; dsRNA, double-stranded RNA; ELISA, enzyme-linked immunosorbent assay; FACS, fluorescence-activated cell sorting; HCV, hepatitis C virus; IFN, interferon; IFNAR, type I IFN-alpha receptor; IL, interleukin; IRF, IFN regulatory factor; MβCD, methyl-beta-cyclodextrin; MDA5, melanoma differentiation associated gene 5; mAb, monoclonal antibody; MoDC, monocyte-derived dendritic cell; MOI, multiplicity of infection; MV, measles virus; NK, natural killer; NKG2D, natural killer group 2, member D; PAMP, pathogen associated molecular pattern; PBMC, peripheral blood mononuclear cells; pDC, plasmacytoid DC; poly I:C, polyinosinic:polycytidylic acid; RIG-I, retinoic acid inducible gene I; RSV, respiratory syncytial virus; RT-PCR, reverse-transcription polymerase chain reaction; siRNA, small interfering RNA; SNARF1, far red immunofluorescence dye; Th1, T helper 1; TLR, Toll-like receptor; TNF, tumor necrosis factor.

From the [1]Department of Microbiology and Immunology, Hokkaido University Graduate School of Medicine, Sapporo, Japan; and [2]Department of Virology II, National Institute of Infectious Diseases, Tokyo, Japan.

Received September 10, 2007; accepted March 11, 2008.

Supported in part by CREST and Innovation, Japan Science and Technology Corporation, the Program of Founding Research Centers for Emerging and Reemerging Infectious Diseases, MEXT, and Grants-in-Aid from the Ministry of Education, Science, and Culture (Specified Project for Advanced Research) and the Ministry of Health, Labor, and Welfare of Japan and the HCV project in National Institute of Health of Japan, and by the Takeda Foundation, Uehara memorial Foundation, Mitsubishi Foundation, Akiyama Foundation, and NorthTec Foundation.

Masashi Shingai is currently affiliated with the Laboratory of Molecular Microbiology, National Institute of Allergy and Infectious Diseases, National Institutes of Health, Bethesda, MD.

Address reprint requests to: Tsukasa Seya, Department of Microbiology and Immunology, Graduate School of Medicine, Hokkaido University, Kita-ku, Sapporo, 060-8638, Japan. E-mail: seya-tu@pop.med.hokudai.ac.jp; fax: 81-11-706-7866.

Published online in Wiley InterScience (www.interscience.wiley.com).

DOI 10.1002/hep.22337

Potential conflict of interest: Nothing to report.